

Predator-scale spatial analysis of intra-patch prey distribution reveals the energetic drivers of rorqual whale super-group formation

David E. Cade^{1,2,*}, S. Mduduzi Seakamela³, Ken P. Findlay^{4,5}, Julie Fukunaga¹, Shirel R. Kahane-Rapport¹, Joseph D. Warren⁶, John Calambokidis⁷, James A. Fahlbusch^{1,7}, Ari S. Friedlaender², Elliott L. Hazen⁸, Deon Kotze³, Steven McCue³, Michael Meyer³, William K. Oestreich¹, Machiel G. Oudejans⁹, Christopher Wilke¹⁰, Jeremy Goldbogen¹

* author to whom correspondence should be addressed: davecade@stanford.edu

¹ Hopkins Marine Station, Stanford University, 120 Ocean View Blvd, Pacific Grove, CA 93950, USA

² Institute of Marine Science, University of California, Santa Cruz, 115 McAllister Way, Santa Cruz, CA 95060, USA

³ Department of Environment, Forestry and Fisheries, Branch: Oceans and Coasts, Victoria & Alfred Waterfront, Cape Town, South Africa

⁴ Oceans Economy, Cape Peninsula University of Technology, Cape Town, South Africa

⁵ MRI Whale Unit, Department of Zoology and Entomology, University of Pretoria, Hatfield, South Africa

⁶ School of Marine and Atmospheric Sciences, Stony Brook University, 239 Montauk Highway, Southampton, NY 11968, USA

⁷ Cascadia Research Collective, Olympia, WA, USA

⁸ Environmental Research Division/Southwest Fisheries Science Center/National Marine Fisheries Service/National Oceanic and Atmospheric Administration, Monterey, CA 93940, USA.

⁹ Kelp Marine Research, 1624 CJ Hoorn, The Netherlands

¹⁰ Department of Environment, Forestry and Fisheries, Branch: Fisheries Management, Foretrust Building, Foreshore, Rogge Bay, Cape Town, South Africa

Acknowledgements: We gratefully thank Duke Marine Robotics and Remote Sensing for UAV images, Tamara Goldbogen for data transfer, John Ryan for contributions related to the spatial locations of super-groups, and the crews of the RV FRS Ellen Khuzwayo and the Moss Landing Marine Labs based RV John Martin. All cetacean data collected under NMFS permits 16111, 20430 and South African permits RES2015/DEA and RES2016/DEA. All procedures were conducted under institutional IACUC protocols. This work funded with NSF IOS grant #1656691, ONR YIP grant #N000141612477, Stanford University's Terman and Bass Fellowships, and funding from the South African Department of the Environment, **This is the author manuscript accepted for publication and has undergone full peer review but has not been through the copyediting, typesetting, pagination and proofreading process, which may lead to differences between this version and the [Version of Record](#). Please cite this article as [doi: 10.1111/1365-2435.13763](https://doi.org/10.1111/1365-2435.13763)**

This article is protected by copyright. All rights reserved

34 Forestry and Fisheries. Monterey bathymetric data provided by MBARI and NOAA's National Centers for
35 Environmental Information. South African bathymetric data provided by the South African Navy
36 Hydrographic Office.

37

38 *Author contributions:* DEC, SMS, KPF, JC, ASF, ELH, & JAG drove investigation. JDW calculated TS
39 of *E. lucens* and *T. spinifera*. DEC, JF & JAG prepared hydroacoustic data for processing. DEC & SRKR
40 analyzed feeding rates from tag data. DEC, SMS, KPF, DK, SM, MM, MGO, CW, JC, ASF, JAF, ELH,
41 SRKR, WKO & JAG collected field data. DEC processed the hydroacoustic and tag data, performed
42 statistical analyses and led the writing of the manuscript. All authors contributed substantially to revisions
43 and gave final approval for publication.

44

45 *Data accessibility:* Prey and tag data have been deposited at Stanford University's digital repository:
46 <https://purl.stanford.edu/rq794kc6747>. Monterey bathymetric data used for Fig. 7 is available publically:
47 <https://www.ncei.noaa.gov/metadata/geoportal/rest/metadata/item/gov.noaa.ngdc.mgg.dem:3544/html>.

49
50
51
52
53
54
55
56
57
58
59
60
61
62
63
64
65
66
67
68
69
70
71
72
73
74
75
76
77
78
79
80

DR DAVID EDMUND CADE (Orcid ID : 0000-0003-3641-1242)

Article type : Research Article

Editor : Functional ecology. Spatial ecology

Section : Dr Daniel Crocker

Predator-scale spatial analysis of intra-patch prey distribution reveals the energetic drivers of rorqual whale super-group formation

Abstract

1. Animals are distributed relative to the resources they rely upon, often scaling in abundance relative to available resources. Yet, in heterogeneously distributed environments, describing resource availability at relevant spatial scales remains a challenge in ecology, inhibiting understanding of predator distribution and foraging decisions.
2. We investigated the foraging behavior of two species of rorqual whales within spatially limited and numerically extraordinary super aggregations in two oceans. We additionally described the lognormal distribution of prey data at species-specific spatial scales that matched the predator's unique lunge-feeding strategy.
3. Here we show that both humpback whales off South Africa's west coast and blue whales off the US west coast perform more lunges per unit time within these aggregations than when foraging individually, and that the biomass within gulp-sized parcels was on average higher and more tightly distributed within super-group associated prey patches, facilitating greater energy intake per feeding event as well as increased feeding rates.
4. Prey analysis at predator-specific spatial scales revealed a stronger association of super-groups with patches containing relatively high geometric mean biomass and low geometric standard deviations than with arithmetic mean biomass, suggesting that the foraging decisions of rorqual whales may be more influenced by the distribution of high-biomass portions of a patch than total biomass. The hierarchical distribution of prey in spatially-restricted, temporally-transient, super-group associated patches demonstrated high biomass and less

81 variable distributions that facilitated what are likely near-minimum intervals between feeding
82 events.

83 5. Combining increased biomass with increased foraging rates implied that overall intake rates
84 of whales foraging within super-groups were approximately double those of whales foraging
85 in other environments. Locating large, high-quality prey patches via the detection of
86 aggregation hot-spots may be an important aspect of rorqual whale foraging, one that may
87 have been suppressed when population sizes were anthropogenically reduced in the 20th
88 century to critical lows.

89

90 Key words: patchiness, krill, gulp-sized cell, lognormal prey distribution, blue whales and humpback
91 whales, social foraging, filter-feeding, fisheries acoustics, foraging ecology, whale scale

92

93 **Introduction**

94 Both the density of foraging predators and the types of collective behaviors displayed by groups
95 are strongly driven across taxa by the heterogeneity, or patchiness, of resources in the environment (Piatt
96 & Methven 1992; Gordon 2014), but effectively describing the availability of patchy resources to foragers
97 is a fundamental challenge in ecology (Levin 1992; Benoit-Bird et al. 2013; Chave 2013). Baleen whale
98 (Mysticeti) systems are an ideal lens through which to study the physiological drivers and ecological
99 limits related to patchiness because, as capital-breeding bulk filter-feeders, they require dense
100 concentrations of seasonally available prey; essentially, their life history is driven by both spatial (Piatt &
101 Methven 1992; Hazen et al. 2009; Hazen, Friedlaender & Goldbogen 2015; van der Hoop et al. 2019) and
102 temporal patchiness (Fossette et al. 2017; Abrahms et al. 2019). Additionally, unusually in pelagic
103 systems it is possible to study both the behavior of baleen whales and the distribution of their euphausiid
104 (krill) prey quantitatively and simultaneously in situ via the use of bio-logging tags and hydroacoustic
105 echosounders (e.g. Baumgartner & Mate 2003; Owen et al. 2017; Goldbogen et al. 2019; Guilpin et al.
106 2019).

107 Baleen whales are the largest predators of all time, and rorqual whales (in the clade
108 Balaenopteroidea) including blue (*Balaenoptera musculus*) and humpback whales (*Megaptera*
109 *novaeangliae*), can engulf volumes of water (means ~ 130 and 15 m³, respectively) that approach or
110 exceed their own body masses (Goldbogen et al. 2012; Kahane-Rapport & Goldbogen 2018). Most
111 typically, lunge filter-feeding whales forage singly or in small groups (≤ 3 animals), and large groups of
112 up to 10-20 animals, often fish-feeding humpback whales, have also been reported in some ecosystems
113 (Jurasz & Jurasz 1979; Whitehead 1983; Kirchner et al. 2018). Group membership can be defined
114 spatially or behaviorally according to the process under study (Mann 2000); here we refer to groups as

115 spatially cohesive aggregations, regardless of social, temporal or behavioral affiliations, such that
116 individuals must interact with each other (constructively or destructively) when accessing prey.
117 Topographical or transient oceanographic features (i.e. bays, fronts and upwelling regions) are sometimes
118 associated with very large numbers (200+) of animals distributed over large (10-70 km) spatial extents
119 that can generally be considered to be foraging independently of each other (e.g. Jaquet 1996; Nowacek et
120 al. 2011). In contrast, our study involves dense aggregations such that individuals could be in direct
121 conflict for the same resource.

122 The formation of spatially constricted, large aggregations of humpback whales in close proximity
123 (numbering upwards of 100 whales within five body lengths) have been observed since 2011 in the
124 Benguela Current upwelling region off the west coast of South Africa in a region where previous studies
125 reported only loose aggregations up to 20 animals (Findlay et al. 2017). Known as super-groups, similarly
126 large aggregations have been reported historically (e.g. Bruce 1915) and the contemporary reemergence
127 of this behavior may be related to the recovery of regional large whale populations above critical
128 thresholds. Findlay et al. (2017) relate that animals in these super-groups are likely foraging, however,
129 group behavior does not necessarily imply optimal behavior (Przybylski et al. 2013), and the proximate
130 causes that inspire such large aggregations have not before been explained.

131 In this study, we examined the prey conditions near, and the foraging behavior of, large
132 aggregations of rorqual whales in two environments: humpback whales in South Africa and blue whales
133 in Monterey Bay off the US west coast (Fig. 1). We hypothesized that the whales observed in super-
134 groups were foraging throughout the environment in which they were observed, but that foraging
135 conditions were of higher quality proximal to super-group observations, suggesting that prey availability
136 is an underlying driver of super-group aggregation. To test this hypothesis, we characterized the prey
137 fields in both environments proximal to foraging whales that were both loosely and densely aggregated by
138 analyzing fisheries acoustics data at spatial scales that match the foraging style of the predators. We show
139 how this method can be used to reveal differences between heavily-foraged patches proximal to large
140 predator aggregations and other patches in the environment that also appear to contain abundant biomass.
141 We additionally used bio-logging tags in both environments to test whether whales in super-groups
142 demonstrated higher feeding rates than whales not aggregated in super-groups. Illuminating the
143 differences in prey conditions between aggregated and non-aggregated whales may not only explain why
144 super-groups form, but may aid understanding about how predators foraging in a patchy environment
145 make decisions about where and when to expend foraging effort.

146

147 **Materials and Methods-**

148 We investigated aggregations of rorqual whales in two eastern boundary-current upwelling
149 ecosystems: humpback whales in the Benguela Current off South Africa's west coast in 2015 and 2016
150 and blue whales in Monterey Bay off the US west coast in 2017 and 2018 (Fig. 1). These aggregations are
151 distinct from other contemporary descriptions of large baleen whale groups in the extraordinary density of
152 animals within a small region of open ocean – in the case of humpback whales including up to 200
153 individuals within regions as small as 200 m on a side (Findlay et al. 2017) – such that animals must
154 interact with each other as they are foraging (Fig. 2, Video S1). While humpback whale super-groups
155 were the specific focus of research efforts in South Africa, large aggregations of blue whales were
156 encountered only twice opportunistically during Monterey Bay field efforts. For detailed field methods,
157 see Appendix S1 in supporting information.

158

159 Foraging behavior

160 In both locations, to examine foraging behavior within and outside of super-groups we attached
161 integrated 3D accelerometer and video tags to whales for time periods of ~ 2 – 20 hrs. Individual feeding
162 events that involve engulfing a mass of water and krill that can exceed the size of the whale (hereafter,
163 "lunges" or "gulps", see Goldbogen et al. 2017) were identified via their kinematic signatures (as in Cade
164 et al. 2016). Foraging behaviors including feeding rate (lunges per hour), inter-lunge interval, foraging
165 bout length, and foraging depth were compared within species between super-group and non-super-group
166 times (details in Appendix S1), as well as between the two study ecosystems and among other ecosystems
167 with krill-feeding whales of the same species (total of 112 blue whales and 45 humpback whales, Table
168 1).

169 To determine the significance of comparisons between super-group and non-super-group foraging
170 of tagged animals, both t-tests and generalized linear mixed effects (GLME) models were used. Foraging
171 of tagged whales when they were and were not in super-groups was compared, and super-group foraging
172 was additionally compared to other whales in the same environment but not in super-groups. Finally,
173 super-group foraging was compared to a larger population of whales outside of the specific tagging
174 period. For humpback whales, this was all krill-feeding whales from CA, the Antarctic and South Africa.
175 For blue whales, this was a comparison with blue whales in the same region as the super-group (Monterey
176 Bay) but a year later. T-tests were used to test for significant differences between mean feeding rates
177 (lunges per hour during foraging bouts) of super-group whales and mean feeding rates of whales foraging
178 when not aggregated in super groups (Tables 2, S2). For both species, foraging bouts were defined as the
179 time period that included all foraging dives with less than 5.5 minutes (see Appendix S1 and Fig. S4)
180 from the return to the surface of one foraging dive to the start of the next foraging dive. GLME models
181 were constructed in Matlab 2019a for inter-lunge interval (ILI), lunges per dive, dive duration and search

182 area from all data using super-group status as a fixed effect and individual whale as a random effect. For
183 dive duration and lunges per dive, factors known to be influenced by dive depth, mean lunge depth for
184 each dive was binned into 50 m depth bins and used as an additional random effect.

185

186 Prey data collection and initial processing

187 Prey data were collected using multi-frequency (38 and either 120 or 200 kHz), split-beam
188 fisheries acoustic systems (Simrad EK60s or EK80s) ensonifying the water column below a vessel within
189 an estimated 500 m of foraging whales in both ecosystems, a distance we considered proximal given the
190 size of observed patches. Data collected near super-groups were compared to data collected near feeding
191 whales not aggregated into super-groups on each observation day and in aggregate as described below.
192 Krill biomass at each analyzed spatial scale was estimated from the mean volume backscattering strength
193 (S_v in dB re $1\text{-m}^2\text{m}^{-3}$, Table 3) of pings aggregated into cells in Echoview v9 with heights and lengths as
194 detailed below. The acoustic set-up, the calculation of target strength for small krill, and the conversion of
195 acoustic units to biomass units are all detailed in Appendix S1. Aggregations of krill, dominated by large
196 swarms > 10 m thick and 1 km across, were identified in Echoview v9 acoustic echograms using the
197 SHAPES school detection algorithm (Barange 1994; Coetzee 2000) and dB differencing techniques
198 (Jarvis et al. 2010, additional details in Appendix S1).

199

200 Predator-scale prey analysis

201 Rorqual whales utilize a unique foraging style, lunge filter-feeding, characterized by raptorial
202 targeting of discrete parcels of water followed by filtration through baleen plates and retention of prey
203 (Pivorunas 1979; Goldbogen et al. 2017). Typically this behavior consists of diving to depths ranging
204 from the surface to > 300 m, performing one to ten lunges, and then returning to the surface to breathe
205 before diving again. To match the spatial scale of prey analysis to the spatial scale utilized by diving
206 whales, we first used tag data to identify the mean horizontal and vertical distances traveled by foraging
207 whales of both study species from 10 s before the first lunge in a dive to 10 s after the last lunge in a dive
208 (distances in Table 1, details in Appendix S1). We then divided the acoustically identified prey patches
209 (Figs. 3A, 4C-D) into these dive-sized cells (Figs. 3B, 4E-F).

210 To examine the distribution of krill within dive-sized cells (Fig. 3C, 4H), we used Echoview to
211 calculate S_v within analytical cells the size of an average whale engulfment volume (S_{v_gulp} , symbol
212 definitions in Table 3) as calculated from the morphology of an intermediately-sized representative of
213 each species of interest (blue whale total length = 22.5 m, humpback whale = 10.5 m). Jaw length was
214 used for the vertical size of the cell (blue whale = 4.3 m, humpback whale = 2.3 m) and the ventral groove
215 blubber length (blue whale = 12.8 m, humpback whale = 6.0 m) was used for the horizontal cell size

216 (lengths calculated from ordinary least squares regression relationships in Kahane-Rapport & Goldbogen
217 2018). At the observed prey patch depths, all return echoes had y-axis values larger than the head width,
218 so the extracted cells represented a 2D projection of the gulp size. The engulfed water volume of rorqual
219 whales is a good spatial match for the analysis of acoustic data since the large size of engulfed water
220 parcels allows multiple acoustic returns to be processed even at our smallest desired spatial scale. Gulp-
221 sized cells contained a minimum of two pings, and in Monterey, blue whale gulp-sized cells averaged 9.4
222 ± 12.5 pings (mean \pm SD), while in South Africa humpback whale gulp-sized cells averaged 8.4 ± 6.8
223 pings (details in Appendix S1). The variation in the number of pings per gulp is a product of variable
224 speeds by the survey vessel and variable ping rates set to maximize the number of samples without
225 introducing acoustic artefacts like false bottoms. When such variation is present in a survey, data that is
226 averaged into patches without first accounting for survey distance can potentially be biased. We report
227 whole patch S_v (e.g. Fig. 4C,D, Table S3) for comparison to the spatially averaged approach described
228 above.

229

230 Characterizing patchy prey

231 In both marine (Bennett & Denman 1985; Campbell 1995) and terrestrial (White 1978)
232 environments, both inter- (Preston 1948; Preston 1962; Pagel, Harvey & Godfray 1991; Magurran &
233 Henderson 2003) and intra- (Barnes 1952; Anand & Li 2001) species abundances tend to be distributed
234 heterogeneously and can often be characterized by lognormal distributions (Dennis & Patil 1987). That is,
235 the log of abundance data is typically normally distributed and can be characterized by the mean and
236 standard deviation of logged data, or, equivalently, the geometric mean and geometric standard deviation
237 of the unlogged data. Fisheries acoustics data, however, are typically reported as overall mean abundance
238 integrated over broad areas (e.g. Croll et al. 1998; Benson et al. 2002; Cox et al. 2009; Nickels, Sala &
239 Ohman 2019) or mean volumetric density within patches (e.g. Nowacek et al. 2011; Hazen, Friedlaender
240 & Goldbogen 2015; Owen et al. 2017). Prey patches can be heterogeneously distributed in space
241 (Watkins & Murray 1998; Kaartvedt et al. 2005; Benoit-Bird, Waluk & Ryan 2019), however, and
242 aggregations themselves can have variable structure (Benoit-Bird, Moline & Southall 2017), implying
243 that using a single number to characterize the biomass density of a large patch may not represent what a
244 foraging animal encounters (Stephens & Krebs 1986). Additionally, averaging the biomass densities
245 among patches with variable sizes may misrepresent mean availability if biomass is not weighted by
246 patch size, or if acoustic surveys with variable ping rates or vessel speeds are not first averaged into
247 spatially consistent regions.

248 When prey patches are small such that a lunge-feeding whale feeds on it only once, describing
249 patch density with a single number for each krill patch would be an appropriate strategy. However, the

250 krill swarms we observed in this study were several km across (Fig. 2) such that predators could be
 251 considered to be foraging within a patch rather than among patches. Consequently, to better represent the
 252 prey biomass available to foraging rorqual whales, we characterized the prey fields proximal to feeding
 253 whales at predator-specific spatial scales, dividing large patches into analytical cells the size of an
 254 individual whale's gulp and then examining how those gulp-sized cells are distributed within cells of a
 255 size likely experienced by whales on a foraging dive (Figs. 3-4). These gulp-sized cells are distributed, as
 256 in patchy prey in other aquatic and terrestrial systems, lognormally (more details in Appendix S1, Fig.
 257 S1). Details for estimating mean intake from lognormal distributions are also reported in the Appendix S1
 258 section "Estimating overall intake."

259

260 The whale scale

261 For each dive-sized cell in a region of interest (e.g. all dive sized-cells proximal to a super-group
 262 on a specific day), we first summarized the distribution of biomasses likely to be experienced by a
 263 foraging whale on a dive by calculating the mean and standard deviation (SD) of S_{v_gulp} within each dive-
 264 sized cell. To ensure sufficient statistical power, only cells that had at least thirty gulp-sized cells were
 265 included in analysis. We then summarized the overall distribution in super-group associated patches and
 266 patches not associated with super-groups by averaging all dive summary values (${}_N S_{v_ws}$) in a region and
 267 calculating the pooled SD of all dives within the region of interest (Fig. 3C). We refer to this summarized
 268 analysis of prey as the mean "whale scale" ($\overline{{}_N S_{v_ws}}$ in acoustic units, $\overline{{}_{LN} B_{WS}}$ in estimated biomass units,
 269 Table 3).

270 All statistical comparisons were done on the acoustic units which have approximately normal
 271 distributions, and then S_v was converted to estimated biomass (generally following Jarvis et al. 2010, with
 272 study system specific calculation details in Appendix S1). Because biomass estimation is subject to model
 273 enhancements over time, we report S_v (as mean \pm pooled SD) throughout the text in addition to biomass
 274 (B, Table 3). Biomass of gulp-sized cells (B_{gulp}) was lognormally distributed at larger scales (Fig. S1), so
 275 for whale-scale summary values we present the geometric mean (geomean) and the geometric standard
 276 deviation (GSD) of gulp-sized cells (B_{gulp}). The geomean and GSD are equivalent to the antilog of the
 277 mean and SD of $\log(\text{biomass})$. There are several advantages to summarizing data using lognormal
 278 distributions instead of reporting mean biomass including less sensitivity to outliers and a better ability to
 279 characterize the spread of data. We report lognormal summary statistics as "biomass in $\text{kg m}^{-3} \bullet\text{:}$ a
 280 multiplicative scalar", where $\bullet\text{:}$ is read "multiplied or divided by" and is a combination of the
 281 multiplication (\bullet) and division (:) symbols introduced by Leibniz (1684). $\bullet\text{:}$ can be interpreted as the
 282 multiplicative complement to the commonly used \pm .

283 The whale scale analytical scale – the distribution of gulp-sized cells within its corresponding
284 dive-sized cell (Fig. 3C, Fig. 4E,F) – can be thought of as the spread of biomass around a dive’s median
285 biomass. We developed this scale because of its link to the spatial scale of prey experienced by foraging
286 rorqual whales on any given foraging dive. This analytical technique gives a representation of what a
287 foraging rorqual could encounter on a dive and would represent what it is likely to forage on if it forages
288 indiscriminately during its dive. However, to account for the likelihood that rorquals employ an active
289 selection strategy to maximize their prey intake we additionally analyzed the distribution of only the top
290 50% of gulp-sized cells within dive-sized cells. The choice of 50% as a threshold was selected as a
291 compromise between indiscriminate feeding centered around a patch’s median and precise selection of
292 gulps with maximum density given how much is unknown about the behavioral patch selection algorithm
293 employed by rorqual whales. We refer to this technique as the “informed whale-scale” analysis and it can
294 be thought of as the distribution of biomass around the 75th percentile of biomass in a dive-sized cell.
295

296

Results

297 Humpback whale super-groups off South Africa’s west coast are described in detail in Findlay et
298 al. (2017) and consist of 20-200 whales surfacing haphazardly in an area as restricted as 200 m on a side
299 (Fig. 2A, Video S1). Super-groups were observed on 10 of 20 ship days in 2015-2016 (Fig. 1). The
300 duration of super-group cohesiveness is unknown as none were observed from formation to dispersal, but
301 all were observed for at least one hour and in all five instances where group dispersion was observed,
302 emigration was sequential. Unlike in other environments where humpback whales have been observed
303 coordinating their fish-feeding behavior (Jurasz & Jurasz 1979; Wiley et al. 2011; Mastick 2016),
304 underwater video evidence suggests that lunge-feeding within these krill patches is uncoordinated (e.g.
305 Video S1). Two blue whale super-groups were encountered in four field days in 2017 in Monterey Bay,
306 California, USA and consisted of an estimated 15-40 whales surfacing within sight of an observer at sea
307 level (~ 1 km range); no super-groups were encountered in nine field days in 2018. Blue whales generally
308 forage in singles or in pairs and the super-groups we observed consisted of many singles and pairs feeding
309 in the same area in an apparently uncoordinated fashion. Due to the similarities in behavior and the much
310 larger sizes of blue whales (blue whales are ~ 2x the length, 4x the mass and have 8x the engulfment
311 capacity of humpback whales, Kahane-Rappoport & Goldbogen 2018) we propose that the observed group
312 sizes are comparable despite their differences in individual predator abundances. The blue whale super-
313 group encountered on Aug 14 (25-40 whales estimated) was encountered at 08:30 and had begun to
314 decrease in density at ~11:15. On Aug 16 the group (15-20 whales estimated) was encountered at 13:30
315 and our vessels left the area at 14:20.

316

317 Foraging behavior

318 All whales fed continuously (accounting for surface recovery and transit time) while in super-
 319 groups. Humpback whales fed at a mean depth of 43 ± 13 m while blue whales fed at 109 ± 30 m (e.g.,
 320 Fig. 2). In both cases, whales in super-groups had similar lunges per dive as non-super-group whales
 321 (Table 2), but the smaller ILI and area traversed between lunges for whales in super-groups compared to
 322 non-super-groups (Table 2) led to shorter dive durations (model estimates accounting for foraging depth
 323 differences, blue whale 95% confidence interval (CI): 197 to 391 s shorter, humpback whale 95% CI: 60
 324 to 112 s shorter). These factors combined to influence the overall feeding rate, as measured in lunges per
 325 hour during feeding bouts, which were 49 and 14% higher, respectively, in humpback whale and blue
 326 whale super-groups vs feeding rates when these same whales were not feeding in super-groups, and were
 327 45 and 34% higher, respectively, when super-group whales were compared to krill-feeding whales more
 328 generally (Table 2). The increased feeding rates in super-groups suggested that we would find that prey
 329 near super-group were distributed in such a way as to facilitate decreased search times.

330

331 Prey analysis

332 Analysis of prey abundance and distribution revealed high-quality foraging conditions in both
 333 super-group and non-super-group behavior states in each ecosystem. Identified prey patches near foraging
 334 whales were typically 10s of m thick and 100s of m wide, regardless of group size, such that whales could
 335 be described as foraging within a patch rather than among patches (Fig. 2, Video S1). Examination of the
 336 distribution of the biomass of gulp-sized cells from all identified patches on each survey day revealed the
 337 biomass density was distributed lognormally (Fig. S1, Appendix S1), suggesting the appropriateness of
 338 the “whale scale” analytical technique for describing the prey field experienced by these large predators.
 339 Describing skewed data using the lognormal parameters (geomean and GSD) has the additional advantage
 340 of being less sensitive to outliers in the data, and summarizing acoustic data into spatially determined
 341 cells has the advantage of matching the spatial scale of collection with the spatial scale experienced by the
 342 predator of interest.

343 In comparing the prey fields in super-group and non-super-group regions, we found that prey
 344 density was generally higher in super-group than in non-super-group regions. On ten of eleven
 345 observation days (Table S3, Fig. 5) geomean prey density at the whale scale ($\overline{LN B_{ws}}$) was higher near
 346 super-groups than near foraging whales not in super-groups ($p < 0.001$ in both environments): blue whale
 347 gulps in super-groups averaged $1.5 \bullet 1.6 \text{ kg m}^{-3}$ ($-47.5 \pm 2.2 \text{ dB}$) while gulps in non-super-groups
 348 averaged $1.2 \bullet 1.8 \text{ kg m}^{-3}$ ($-48.5 \pm 2.6 \text{ dB}$), and humpback whale gulps in super-groups averaged $0.49 \bullet$
 349 2.0 kg m^{-3} ($-50.7 \pm 3.0 \text{ dB}$) while non-super-group gulps averaged $0.31 \bullet 2.1 \text{ kg m}^{-3}$ ($-52.7 \pm 3.3 \text{ dB}$). In

350 three of eleven days, prey density was lower near super-groups if prey was described using whole patch
351 means (further discussed below). Patches were additionally substantially and significantly thicker near
352 super-groups in all cases (mean in South Africa: 22 ± 14 m vs 8 ± 9 m, mean in Monterey: 33 ± 27 m vs
353 15 ± 15 m, Fig. 5, Table S3).

354 The GSD of gulps at the mean whale scale was not significantly different between super-groups
355 and non-super-group patches on any given day (Table S3). In 9 of 10 cases the mean gulp at the mean
356 informed whale scale (i.e., the mean gulp within the denser half of dive-sized cells) was significantly
357 higher in super-groups, and in all cases the SD of gulp density at the informed whale scale was 0.1-0.6 dB
358 lower in super-groups than non-super-groups.

359 Prey conditions in the same region both before and during super-group formation were observed
360 just once in South Africa on 05 Nov 2015 (Fig. 4, Fig. 6). In that case, 150-200 whales were spread out
361 along a shelf break before coming together into a single aggregation (Fig. 6). Prey density in patch
362 averages was not significantly different before or during super-group formation ($p > 0.9$, Fig. 5).
363 However, the geomean of gulps at the mean whale scale was 38% higher ($p = 0.010$) in super-group
364 associated patches and was 21% higher at the mean informed whale scale ($p = 0.002$). Additionally, mean
365 patch thickness was estimated to be 14 m larger in super-groups ($p < 0.001$), and gulp GSD at both the
366 whale scale and the informed whale scale was smaller in super-groups, though only significantly so at the
367 informed whale scale (Fig. 5, Table S3).

368 In Monterey Bay, the blue whale super-group on 14 Aug 2017 had a similar pattern as the 05 Nov
369 2015 humpback whale super-group (Fig. 5). While the geomean of patch biomass was smaller (but not
370 significantly different) in the prey field near the observed super-group, geomean gulp biomass at the mean
371 whale scale and the mean informed whale scale were both significantly and substantially higher (Fig. 5,
372 Table S3), and patch thickness and gulp GSD at the informed whale scale were significantly higher and
373 lower, respectively ($p < 0.001$ in both cases, Table S3). While the super-group associated patch on 16 Aug
374 2017 had slightly higher geomean biomass at the whale scale and in patches, results were non-significant
375 (Table S3). Instead, prey around this super-group was characterized by a 2.5-fold increase in patch
376 thickness as well as both a significant increase in geomean gulp biomass density and significant reduction
377 in gulp GSD at the informed whale scale (Table S3).

378 Patches near super-groups thus had more available biomass on average than patches near whales
379 not in super-groups. In both environments, better quality of super-group patches was indicated by higher
380 geomean gulp density, thicker patches and indications that the prey at the informed whale scale (the
381 denser half of the prey in each dive-sized cell) was more uniform in distribution (i.e. displayed smaller
382 variance).

383

384 Discussion

385 Our results suggest that the formation of super-groups of two species of rorqual whales was
386 largely influenced by high-quality foraging conditions. Gulp-sized cells analyzed at the whale scale had
387 higher geomean biomass and lower variability within prey patches associated with super-groups of
388 humpback and blue whales, and whales within super-groups demonstrated higher feeding rates than more
389 dispersed individuals. Furthermore, characterizing the intra-patch distribution of krill biomass appears to
390 offer an explanation for the higher feeding rates observed in super-groups. Specifically, we found that
391 super-groups were strongly associated with patches characterized by high geomeans and low GSD of
392 biomass, particularly in the densest half of gulps within dive-sized cells (the informed whale scale).
393 Higher geomeans implies that even a naïvely foraging whale would benefit from increased energy intake
394 at each feeding event, and a lower GSD (when paired with a high geomean) implies that a greater
395 proportion of gulp-sized parcels would be of sufficient quality to feed (i.e., a greater proportion of gulps
396 were above a threshold at which it would be beneficial to feed), enabling the observed increase in lunge
397 feeding events per unit time by decreasing search time. The match of predator behavior (increased feeding
398 rates) with our findings of higher density with less variance in cells the size of what a predator will
399 experience on a foraging dive additionally supports the whale scale level of analysis.

400 In ecological models of foraging in patchy environments, patch quality is often assessed as the
401 overall intake (per unit time) enabled by an ecosystem (Giraldeau & Caraco 2000). To improve the
402 efficacy of such models, the intake rate parameter, λ , could further be decomposed into two component
403 parts: 1) the energetic quality of each captured prey parcel and 2) the rate at which prey are captured. In
404 rorqual whale foraging systems, these quantities are represented by the mean biomass density in each gulp
405 (λ_p) and the lunge rate per unit time (λ_f), respectively, such that $\lambda = \lambda_p \times \lambda_f$. We found that prey patches
406 associated with super-groups not only had 40-50% more biomass in the median (geomean) gulp than
407 patches not associated with super-groups, implying higher λ_p , but also had smaller GSD. The small GSD
408 implied that prey was of more uniform quality proximal to super-groups, making it easier for whales to
409 maximize consumption without spending time between lunges searching for the best nearby parcel. This
410 reduction in search time likely facilitated the observed increases in super-group λ_f by decreasing the inter-
411 lunge interval as well as the spatial distance traveled between lunges (Table 2). Indeed, the reported
412 super-group feeding rates in both study areas (humpback whales: 55 ± 15 lunges/hr, blue whales: 24 ± 2.9
413 lunges/hr, Table 2) are comparable to the highest reported rates for whales in other studies: Goldbogen et
414 al. (2008) report that one tagged humpback whale fed at a rate of 45 lunges/hr over 8 hrs, Owen et al.
415 (2017) report humpback feeding rates of 49 lunges/hr, while Southall et al. (2019) report blue whale
416 feeding rates over 10 minute bins that range from 5 to 30 lunges/hr when foraging, with mean rates
417 typically less than 20 lunges/hr and max rates over foraging bout-comparable time scales of

418 approximately 25 lunges/hr. The high rates of foraging in super-groups suggests that these whales are
419 feeding at rates close to their biomechanical limits.

420 The analysis of prey at the nested scales we describe is particularly well-suited for describing
421 prey conditions available to krill-feeding rorqual whales because their foraging style utilizes
422 characteristics of both filter-feeding, where energy cost per foraging event is independent of the quality of
423 the prey, and raptorial feeding in which prey (i.e. in bulk patches) are engulfed in discrete units. The
424 combination of these feeding modes distinguishes rorquals from right whales (*Eubalaena glacialis*),
425 whale sharks (*Rhinocodon typus*) and other continuous ram filtration feeders. From our meta-analysis of
426 data from 45 blue whales and 21 humpback whales that lunged multiple times per dive and for which
427 georeferenced tracks could be calculated, we found that those two species traverse an average of 177 ± 51
428 and 73 ± 34 horizontal meters between lunges and average 4.1 ± 1.4 and 5.2 ± 2.3 lunges per dive,
429 respectively, yet the distance traveled for one lunge is only the length of the buccal cavity (12.8 and 6.0
430 m, respectively, for a 22.5 m blue whale and 10.5 m humpback whale). Right whales, approximately the
431 same length as humpback whales, are continuous ram filtration filters that filter an average of 670 m^3 of
432 water on every dive (van der Hoop et al. 2019). At 14 m^3 of water engulfed per lunge (Kahane-Rapport &
433 Goldbogen 2018), a humpback whale would have to lunge 48 times per dive (an order of magnitude more
434 than their average) to filter an equivalent volume. These factors, combined with the ability to feed on
435 more maneuverable prey enabled by high-speed, raptorial approaches (Cade et al. 2020), imply that
436 rorqual whales may be energetically required to make active choices regarding what patch and what part
437 of a patch to feed on, further supporting analysis at the informed whale scale.

438 Matching the spatial scale of analysis to the scale of the event under study is particularly critical
439 in patchy environments (Levin 1992; Benoit-Bird et al. 2013). Although the sensory mechanisms by
440 which rorqual whales determine patch quality in the environment is currently unknown, insights into the
441 process can be gleaned by proposing and examining potential behavioral algorithms used by whales to
442 maximize their energy intake (Hein et al. 2020). Prior work has proposed that baleen whales initiate
443 foraging when prey is available above a certain density (Mayo & Marx 1990; Cotté & Simard 2005;
444 Hazen et al. 2009; Feyrer & Duffus 2015; Kirchner et al. 2018). Our findings extend these ideas by
445 suggesting that the density and distribution of encountered prey is a better indicator of where whales
446 forage than overall patch or regional abundance. Future work may be able to refine this general principle
447 into a prediction for a behavioral algorithm that would describe under what conditions a whale would give
448 up foraging in one environment to take advantage of an environment it perceives as more favorable.

449 Better matching the scale of prey distribution to the scale of predator foraging effort could also be
450 used to better predict overall intake rates (λ). Considering that super-groups of two species of whales
451 aggregated in regions with less variability in the densest half of the cell, and given that rorquals are likely

452 not feeding indiscriminately, we suggest that the actual prey consumed by foraging rorqual whales would
453 likely be reflected by the biomass of prey available at the whale scale as a lower bound, but be even better
454 reflected by analysis at the informed whale scale, and we include suggestions for the calculation of these
455 bounds in Appendix S1. Additional studies to quantify a more precise threshold for the informed whale
456 scale could eventually shed light on how rorquals maximize their foraging efficiency in a given
457 environment.

458 Although humpback and blue whale super-groups have only been recently described, abnormally
459 large densities of krill do not appear to be a new phenomenon. Nicol et al. (1987) report surface swarms
460 of *E. lucens* near our study area in South Africa of up to 35 kg m^{-3} . The historical record of super-groups
461 (Bruce 1915) followed by a lack of observed occurrences during periods of low cetacean abundance
462 combined with consistent aggregations of krill suggest that rorqual whale super-groups were once a more
463 common occurrence. Given the 20%-60% increase in geomean prey density we found in super-groups
464 and the concurrent 33-45% increase in feeding rates compared to non-super-group environments, it is
465 likely that super-groups were once an important part of rorqual whale foraging ecology before
466 anthropogenic hunting removed more than three million whales globally (Rocha, Clapham &
467 Ivashchenko 2014). It is plausible, therefore, that recovering populations benefit from a positive feedback
468 loop whereby increased population sizes increase the likelihood of discovering extensive but ephemeral
469 (Fig. 7) patches since concentrations of calling whales, even if calling is not directly related to patch
470 quality or extent, could serve as a signpost for wanderers about the location of ephemeral high-quality
471 foraging grounds (Wilson et al. 2018). This socially-mediated information exchange would decrease the
472 search time of individuals who might not otherwise find the highest quality regions within a foraging
473 ground (LaScala-Gruenewald et al. 2019; Hein & Martin 2020).

474 The spatial colocation of the observed super-group associated patches with bathymetric features,
475 including small scale (1-5 km wide) canyons that incise typical rorqual foraging habitat regions off the
476 edges of continental shelves (Figs 1, 6, 7), suggest that the two environments in our study may have a
477 specific proclivity to support large, dense prey patches due to the interaction of bathymetry and local
478 oceanographic process that have been shown to aggregate zooplankton (e.g. Santora et al. 2018; Benoit-
479 Bird, Waluk & Ryan 2019). Future work examining the spatiotemporal links between mesoscale
480 oceanographic processes, local bathymetry, and temporally transient prey conditions may better help
481 explain how these large predators effectively exploit prey in spatially and temporally complex habitats.

482 It was not until relatively recently in the fossil record (5-7 Ma) that baleen whales developed
483 gigantic body sizes ($> 10 \text{ m}$), and it is likely that this large change came about in concert with oceanic
484 conditions that favored annually consistent upwelling zones that brought nutrient-rich water to the surface
485 in specific areas, creating natural aggregation areas (Slater, Goldbogen & Pyenson 2017). Locating and

486 exploiting these prey hotspots is essential to the foraging strategy of rorqual whales, and we found that
487 differentiating the highest quality prey areas (as characterized by high geometric means and low GSD)
488 from merely good prey areas can result in a doubling of intake rates (λ) when increased feeding rates (λ_f)
489 are combined with increased prey density (λ_p). We have described two disparate environments in which
490 predator patchiness – indicated by temporally transient and spatially limited super-group formation – is
491 driven by prey patchiness, and we utilize predator-specific prey density metrics to characterize high-
492 quality whale habitat. Our results suggest that foregoing local foraging within good prey environments in
493 favor of traversing to great prey environments where conspecifics are aggregating may be an
494 evolutionarily stable strategy when such prey patches are extensive and ephemeral, and future research
495 may reveal the specific social drivers that cue whales into the locations of these high-quality foraging hot
496 spots.

497

498 **Supporting Information**

499 Additional supporting information may be found in the online version of this article.

500 Appendix S1- Detailed methods

501 Figure S1- Distribution of gulp-sized cells of acoustic energy and biomass for each day

502 Figure S2- Comparisons of bottom echo strength in adjacent regions of varying water column echos

503 Figure S3- Plots of S_a for each 200 kHz ping on 05 Nov 2015

504 Figure S4- Surface interval between foraging dives for blue whales and humpback whales tagged in
505 multiple ecosystems

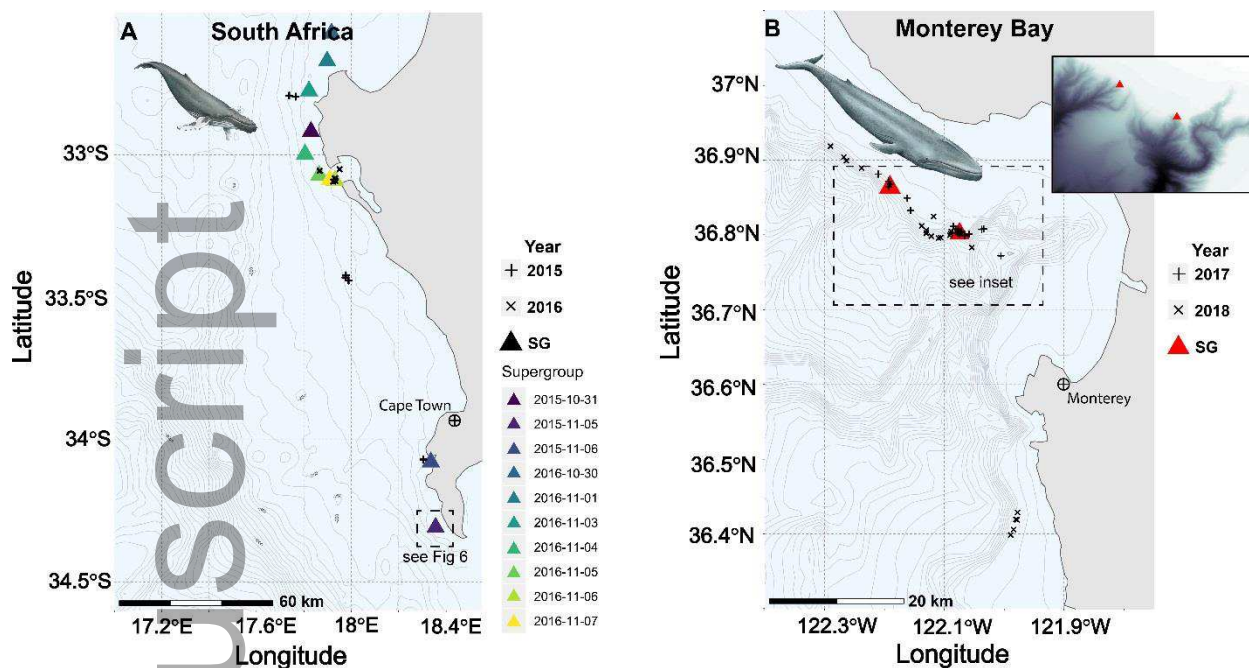
506 Table S1- Summary of data collected near super-groups

507 Table S2- Feeding parameters from tag data for individual whale

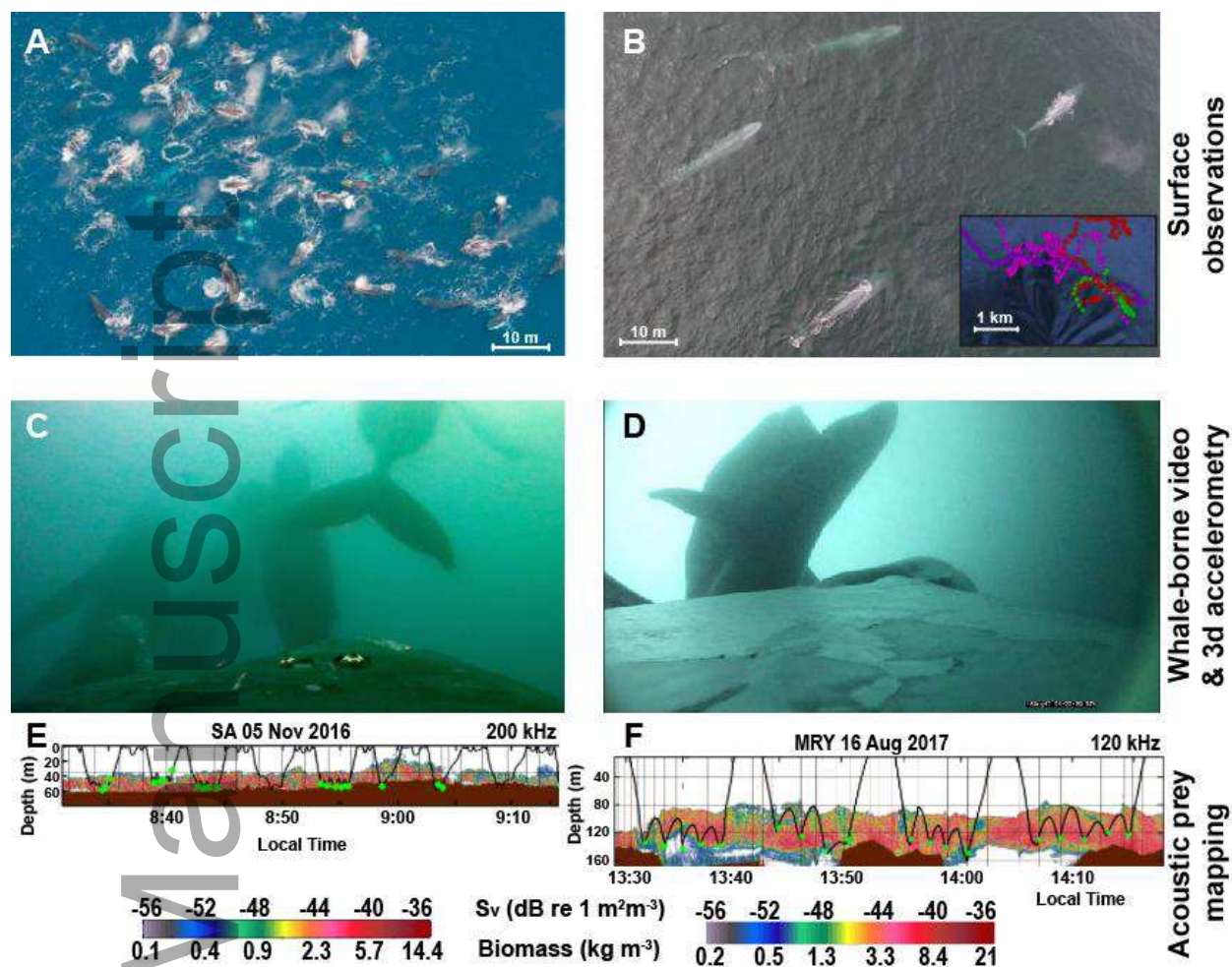
508 Table S3- Summary prey data from each day with super-group observations

509 Video S1- On animal video from humpback whales foraging within super-groups, high quality version
510 available with deposited data at: <https://purl.stanford.edu/rq794kc6747>

511 **Figure legends & Tables**

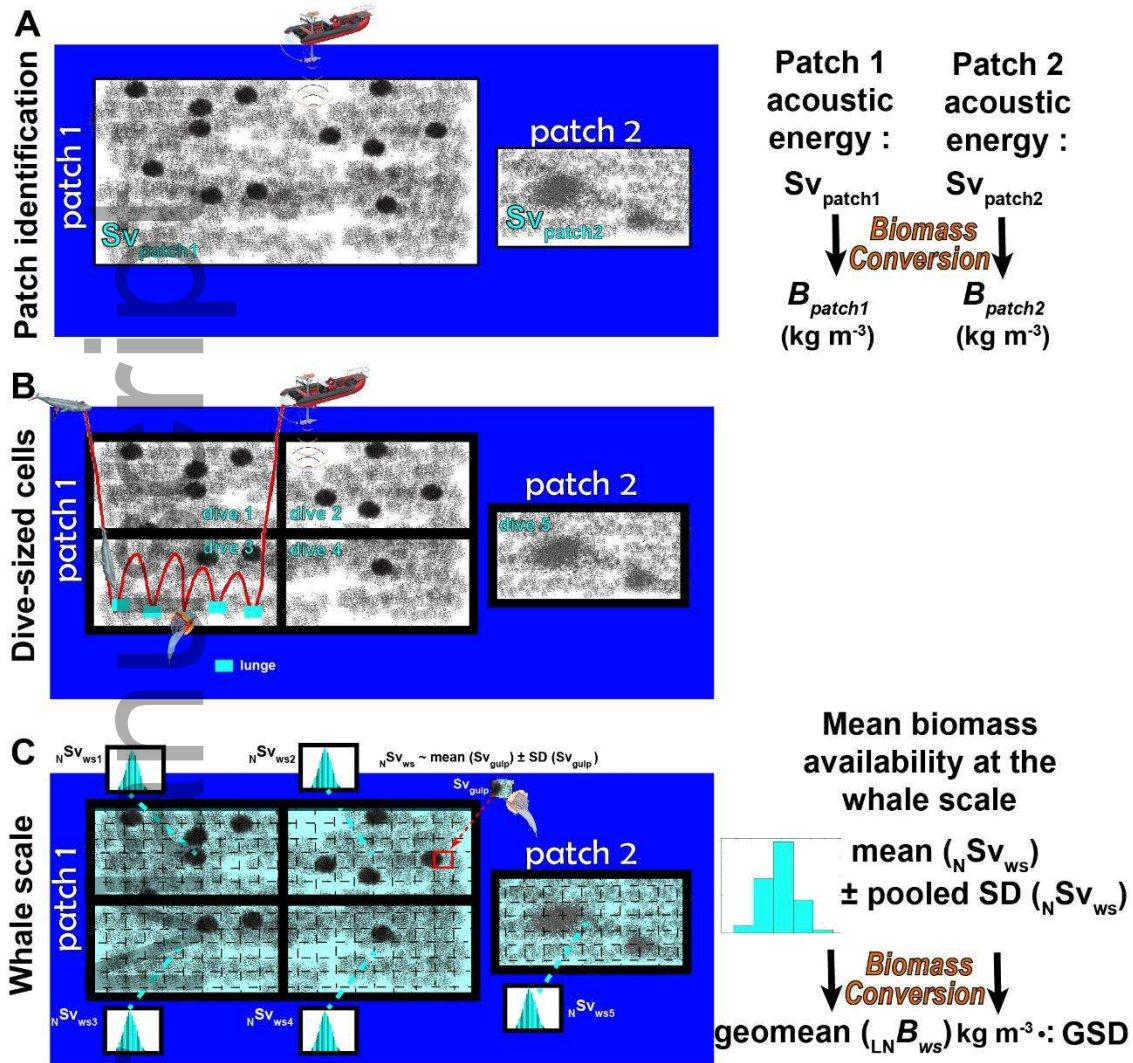


512
 513 **Fig. 1-** Field locations in South Africa (A) and Monterey Bay (B). Depth contour lines are separated by
 514 50 m until the 500 m isobath and then 100 m thereafter. Triangles show observed super-group (SG)
 515 locations, and + and × mark the deployment locations of suction-attached bio-loggers on humpback (A)
 516 and blue whales (B). Data collected near each super-group is collated in Table S1.
 517



518
 519 **Fig. 2-** Investigating super aggregations of predators and prey A) UAV image of at least 60 humpback
 520 whales off South Africa's west coast, scale is estimated from mean humpback whale length (image ©
 521 Jean Tresfon). B) UAV image of four blue whales in an aggregation of ~15 whales in Monterey Bay, CA
 522 (image © Duke Marine Robotics and Remote Sensing). Inset: map of super-group region with tracks of
 523 tagged whales; the green track represents the topmost whale in the image. C&D) Underwater views of
 524 multiple humpback and blue whales, respectively, feeding simultaneously. E&F) Acoustic backscatter
 525 near super-group in South Africa and Monterey Bay, respectively, overlaid with the time-synched depth
 526 profiles and lunges (green circles) of whales tagged nearby. Grid lines are sized to match the dive-scale
 527 unit of analysis for each species.

528



529

530 **Fig. 3-** Schematic illustrating the analytical technique for two acoustically detected prey patches. A) The

531 patch scale is commonly reported in acoustics literature, looking at the linearly averaged mean biomass

532 within each patch. B) In the whale scale approach, patches are first divided into cells the size of an

533 average whale foraging dive (Table 1). C) The whale scale looks at the distribution of the biomass of

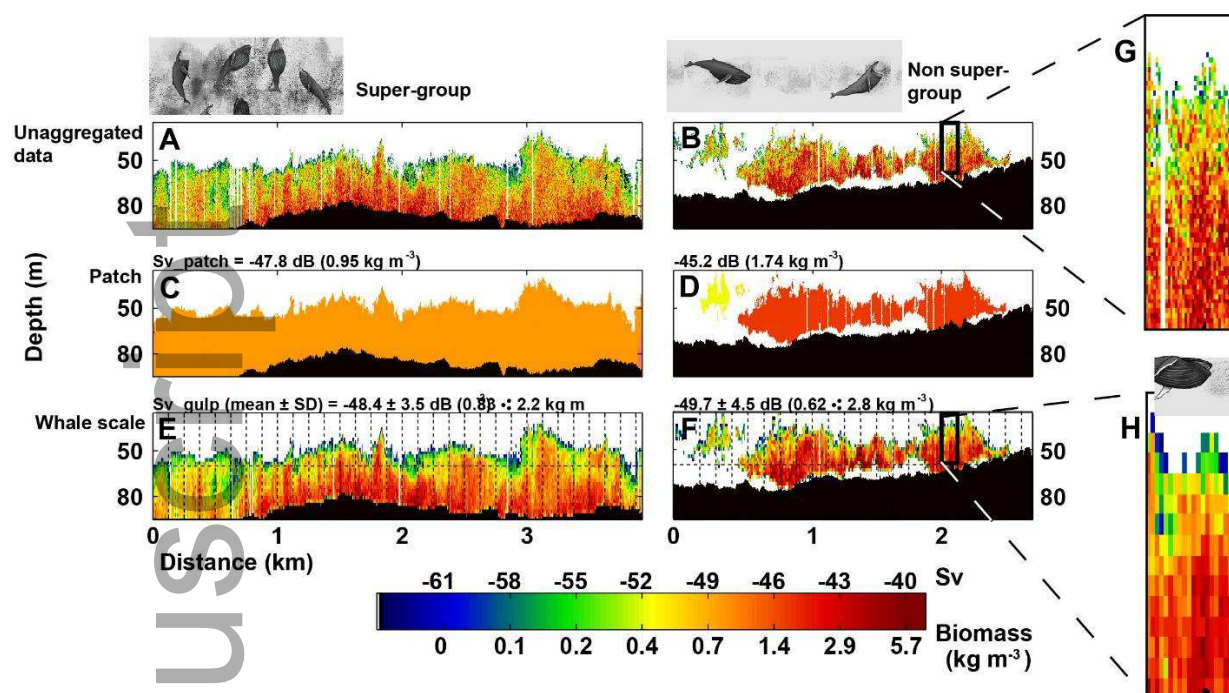
534 gulp-sized cells within dives and then pools results for a representation of the mean availability of

535 biomass at the scale experienced by the predator. Biomass conversion equation in Appendix S1, eq. 1.

536 SD = standard deviation, geomean = geometric mean = antilog(mean(log(biomass))), GSD = geometric

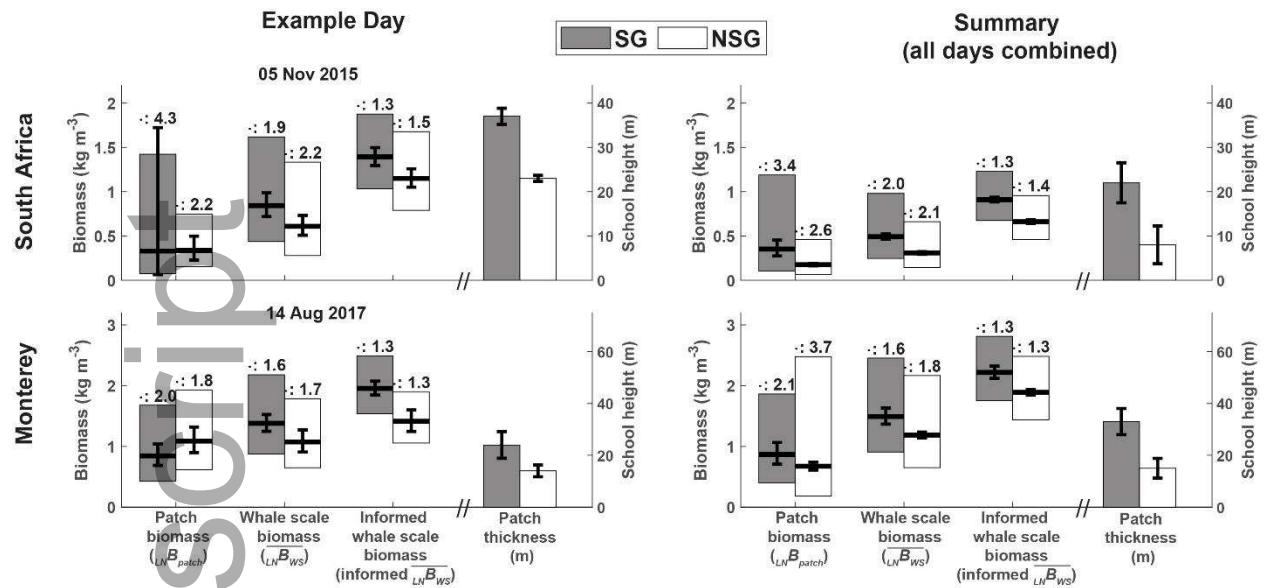
537 standard deviation = antilog(SD(log(biomass))). Other symbols defined in Table 3.

538



539
 540 **Fig. 4-** Matching the spatial scale of rorqual whale feeding with acoustic analysis can illuminate
 541 differences between patches that appear to be of similar quality. A&B) hydroacoustic data from super-
 542 group and non-super-group regions on 05 Nov 2015, averaged into 1 m x 1 m cells (for display purposes
 543 along a consistently sized x-axis). C&D) The mean density of each identified krill swarm as exported
 544 from Echoview. The large non-super-group krill swarm in D had nearly double the krill density overall
 545 than the swarm in C proximate to a super-group, suggesting that the mean density of krill swarms may not
 546 be an appropriate metric to describe prey availability here since at this scale the super-group patch would
 547 appear to be lower quality. E&F) The whale scale: the patch is divided into cells the average size of a
 548 (2D) humpback whale foraging dive (125 m x 35 m) and then further divided into gulp-sized cells. The
 549 geometric mean of the gulp-sized cells within dive-sized cells is higher in the super-group proximal patch.
 550 G) acoustic data in a dive-sized cell at fine resolution. H) acoustic data in a dive-sized cell averaged into
 551 gulp-sized cells, demonstrating how at this resolution the distribution of krill within the patch is
 552 preserved.

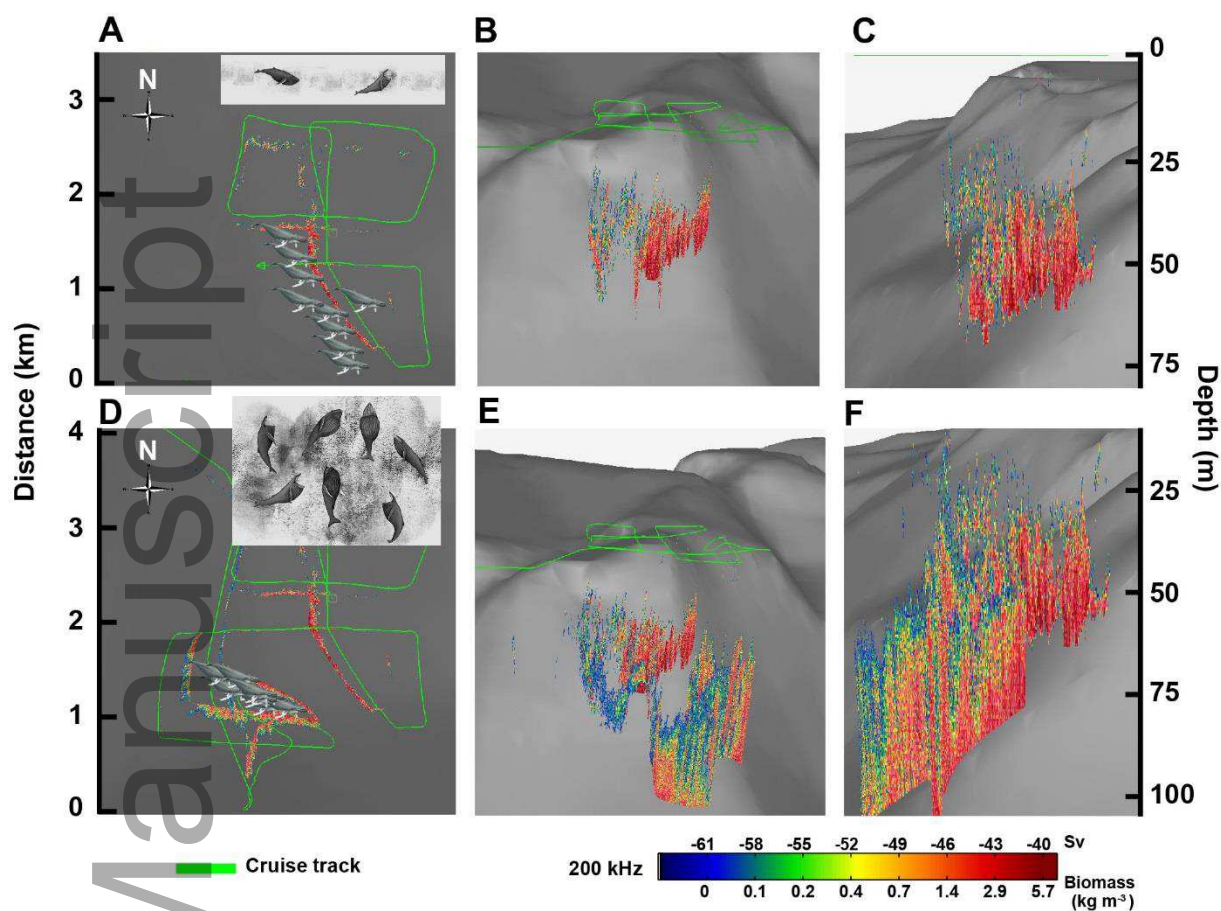
553



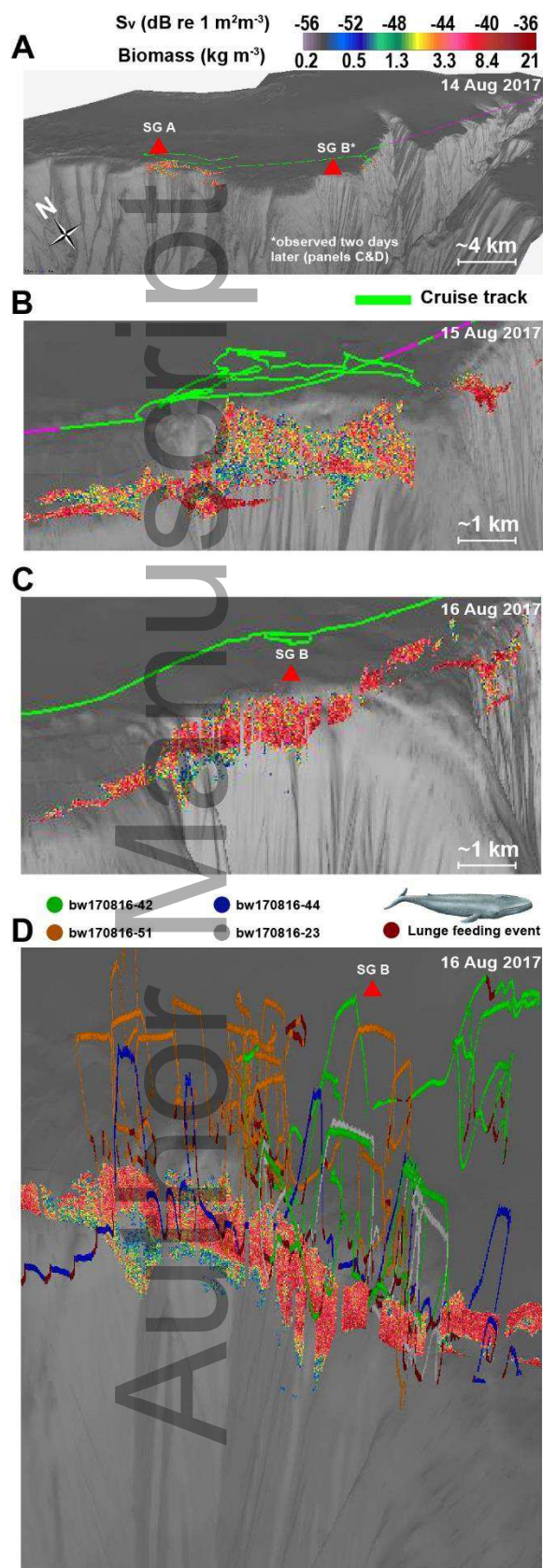
554

555 **Fig. 5-** Summary prey data from an example day and in aggregate for both South Africa and Monterey.
 556 Summary data for all days is displayed in Table S3. Symbol definitions in Table 3, SG = super-group,
 557 NSG = non-super-group. Prey patch geometric means are the thick horizontal bars, and the large bars
 558 represent the GSD with the multiplicative factor listed above each bar. Error bars around the geometric
 559 means are the 95% confidence intervals (calculated in acoustic units and converted to biomass). Patch
 560 thickness error bars are 95% confidence intervals.

561



562
 563 **Fig. 6-** 3d view of super-group associated prey patch on 05 Nov 2015 in South Africa (the southernmost
 564 group in Fig. 1). These are the same data from which Fig. 4 was created. A-C) prey and whales spread out
 565 before super-group formation (prey data shown until 17:00 local time). A) overhead view. B) Oblique
 566 view (from the northwest), highlighting the prey in relation to submarine canyon bathymetry. C) Side-on
 567 view, looking from the south. D-F) Same views now including super-group-associated data when 150-200
 568 whales converged into a region ~ 200 m on a side at ~17:00. Bad weather on this day precluded suction-
 569 cup tag deployment. Whale illustrations by Alex Boersma. Bathymetry courtesy of the South Africa Navy
 570 Hydrographic Office. Data plotted in Echoview v10 using a 50x vertical exaggeration.
 571



573 **Fig. 7-** 3d view of super-group (SG) associated
 574 prey patches in Monterey Bay, CA, USA. A)
 575 Overall layout of the north Monterey Canyon
 576 edge with prey data near SG A on 14 Aug 2017.
 577 B) zoomed in plot of the SG B location, but the
 578 day before the SG was noticed. There were
 579 scattered blue whales feeding in this area, but it
 580 is noticeable how much less uniform and diffuse
 581 the high-quality parts of this large patch are. C)
 582 zoomed in plot of the SG B associated patch on
 583 16 Aug 2017. D) view from the southeast of the
 584 same patch, overlain with tracks from the four
 585 tagged whales feeding within SG B. Data plotted
 586 in Echoview v10 using a 10x vertical
 587 exaggeration.
 588 .
 589

572

590 **Table 1-** Morphometric and feeding parameters that informed analysis, using all krill feeding whales
 591 from (Goldbogen et al. 2019). Body lengths are representative of whales in the region. Ventral Groove
 592 Blubber length (VGB_L) and jaw length (Jaw_L) were allometrically determined (Kahane-Rapport &
 593 Goldbogen 2018) and used to create the gulp-size cell (Figs 3&4). Search areas were used to calculate the
 594 size of the dive-sized cells. ILI = Inter-lunge interval

595

Species	Length	VGB _L	Jaw _L	Vertical search area	Horizontal search area	ILI	Lunges per dive	Deployments
<i>B. musculus</i>	22.5 m	12.8 m	4.25 m	44 ± 16 m [†]	240 ± 119 m [†]	108 ± 254 s	3.3 ± 2.0	112
<i>M. novaeangliae</i>	10.5 m	6.0 m	2.25 m	35 ± 20 m	125 ± 99 m	43 ± 12 s	3.2 ± 1.1	45

596 † Search areas for *B. m.* were limited to deployments with georeferenced pseudotracks ($n = 51$)

597 **Table 2-** Mean feeding parameters derived from tag data for whales foraging in super groups (SG) and
 598 not in super groups (NSG). Feeding bout definition described in Fig. S4. Data for individual whales
 599 foraging in super-groups ($n = 6$ in both ecosystems) in Table S2. *M. n.* = *M. novaeangliae* (humpback
 600 whales), *B. m.* = *B. musculus* (blue whales).

601

* = $p < .05$, ** = $p < .01$, *** = $p < .001$

M. novaeangliae (South Africa)

	Feeding rate (lunges per hr within a foraging bout)		Inter lunge interval (ILI, s)		Inter lunge search area (10^2 m^2)		Lunges per dive	
	SG	NSG	SG	NSG	SG	NSG	SG	NSG
SG animals (p-value)	55 ± 15	37 ± 18	32 ± 10	40 ± 18	3.4 ± 2.5	8.1 ± 11	4.5 ± 1.5	3.6 ± 2.2
number of animals	6	5	6	5	6	3	6	5
All SA <i>M. n.</i> (p-value)	55 ± 15	39 ± 15	32 ± 10	36 ± 16	3.4 ± 2.5	6.6 ± 10	4.5 ± 1.5	4.1 ± 2.5
number of animals	6	7	6	7	6	5	6	7
All <i>M. n.</i> (p-value)	55 ± 15	38 ± 16	32 ± 10	44 ± 18	3.4 ± 2.5	11 ± 26	4.5 ± 1.5	4.4 ± 2.1
number of animals	6	17	6	33	6	30	6	33

B. musculus (Monterey Bay)

	SG	NSG	SG	NSG	SG	NSG	SG	NSG
SG animals (p-value)	24 ± 2.9	21 ± 5.1	95 ± 17	102 ± 19	36 ± 34	42 ± 40	4.0 ± 0.9	3.3 ± 1.3
number of animals	6	5	6	5	6	5	6	5
All MRY 2017 <i>B. m.</i> (p-value)	24 ± 2.9	22 ± 3.9	95 ± 17	101 ± 16	36 ± 34	42 ± 32	4.0 ± 0.9	3.3 ± 1.3
number of animals	6	17	6	17	6	17	6	17
SG <i>B. m.</i> vs 2018 <i>B. m.</i> (p-value)	24 ± 2.9	18 ± 3.1	95 ± 17	108 ± 22	36 ± 34	57 ± 85	4.0 ± 0.9	4.8 ± 1.4
number of animals	6	22	6	22	6	22	6	22

602
603

604
605
606
607
608
609
610

Table 3- Definitions of symbols and abbreviations. See Fig. 3 for schematic representation of hierarchical prey distribution calculations. Subscripts LN or N before the variable denote lognormal or normal distributions, respectively. See MacLennan, Fernandes and Dalen (2002) for further descriptions of S_v and TS. For further discussion of the calculation of \hat{B} or \widehat{S}_v , see Appendix S1 section “Estimating overall intake.” See eq. 1 in Appendix S1 for information on calculating B from S_v

Symbol	Definition	Units	Scale
$\cdot\cdot$	Multiply or divide (the multiplicative correlate to \pm)	–	–
B_{gulp}	Biomass density within a gulp-sized cell	kg m^{-3}	Gulp
B_{patch}	Arithmetic mean biomass density within a patch (estimated from $S_{v_{\text{patch}}}$)	kg m^{-3}	Patch
${}_{\text{LN}}B_{\text{ws}}$	Whale-scale biomass: the distribution of B_{gulp} within a dive-sized cell, estimated from ${}_{\text{N}}S_{v_{\text{ws}}}$ and equivalent to $\text{geomean}(B_{\text{gulp}}) \cdot\cdot \text{GSD}(B_{\text{gulp}})$	kg m^{-3}	Dive
${}_{\text{LN}}\overline{B}_{\text{ws}}$	Distribution of ${}_{\text{LN}}B_{\text{ws}}$ within a patch or region, estimated from ${}_{\text{N}}S_{v_{\text{ws}}}$ and equivalent to $\text{geomean}({}_{\text{LN}}B_{\text{ws}}) \cdot\cdot \text{GSD}({}_{\text{LN}}B_{\text{ws}})$	kg m^{-3}	Patch or region
\hat{B}	Estimated arithmetic mean biomass (mean biomass consumed over time) calculated the summary variables $\text{geomean}(B_{\text{ws}})$ and $\text{GSD}(B_{\text{ws}})$.	kg m^{-3}	Dive, patch or region
geomean	geometric mean	–	–
GSD	Geometric standard deviation	–	–
SD	Standard deviation	–	–
S_v	Mean volume back scatter strength (MVBS)	$\text{dB re } 1 \text{ m}^2 \text{ m}^{-3}$	–
$S_{v_{\text{gulp}}}$ or $S_{v_{\text{gulp}}}$	MVBS within a gulp-sized cell	$\text{dB re } 1 \text{ m}^2 \text{ m}^{-3}$	Gulp
$S_{v_{\text{patch}}}$ or $S_{v_{\text{patch}}}$	MVBS within a patch	$\text{dB re } 1 \text{ m}^2 \text{ m}^{-3}$	Patch
$S_{v_{\text{dive}}}$ or $S_{v_{\text{dive}}}$	MVBS within a dive-sized cell	$\text{dB re } 1 \text{ m}^2 \text{ m}^{-3}$	Dive
${}_{\text{N}}S_{v_{\text{ws}}}$ or ${}_{\text{N}}S_{v_{\text{ws}}}$	Whale-scale S_v : the distribution of $S_{v_{\text{gulp}}}$ within a dive-sized cell, presented as $\text{mean}(S_{v_{\text{gulp}}}) \pm \text{SD}(S_{v_{\text{gulp}}})$	$\text{dB re } 1 \text{ m}^2 \text{ m}^{-3}$	Dive
${}_{\text{N}}\overline{S}_{v_{\text{ws}}}$ or ${}_{\text{N}}\overline{S}_{v_{\text{ws}}}$	Distribution of $\text{mean}({}_{\text{N}}S_{v_{\text{ws}}})$ of all dive-sized cells within a patch or region, presented as $\text{mean}({}_{\text{N}}S_{v_{\text{ws}}}) \pm \text{SD}({}_{\text{N}}S_{v_{\text{ws}}})$	$\text{dB re } 1 \text{ m}^2 \text{ m}^{-3}$	Patch or region
\widehat{S}_v	Estimated MVBS from a dive, patch or region, calculated from the summary variables $\text{mean}(S_v)$ and $\text{SD}(S_v)$	$\text{dB re } 1 \text{ m}^2 \text{ m}^{-3}$	Dive, patch or region
TS	Target strength (see eq. 1 in Appendix S1)	$\text{dB re } 1 \text{ m}^2 \text{ m}^{-3}$	–

611
612
613

614 **References**

- 615 Abrahms, B., Hazen, E.L., Aikens, E.O., Savoca, M.S., Goldbogen, J.A., Bograd, S.J., Jacox, M.G., Irvine,
616 L.M., Palacios, D.M. & Mate, B.R. (2019) Memory and resource tracking drive blue whale
617 migrations. *Proceedings of the National Academy of Sciences*, **116**, 5582-5587.
- 618 Anand, M. & Li, B. (2001) Spatiotemporal dynamics in a transition zone: patchiness, scale, and an
619 emergent property. *Community Ecology*, **2**, 161-169.
- 620 Barange, M. (1994) Acoustic identification, classification and structure of biological patchiness on the
621 edge of the Agulhas Bank and its relation to frontal features. *South African Journal of marine
622 science*, **14**, 333-347.
- 623 Barnes, H. (1952) The use of transformations in marine biological statistics. *ICES Journal of Marine
624 Science*, **18**, 61-71.
- 625 Baumgartner, M.F. & Mate, B.R. (2003) Summertime foraging ecology of North Atlantic right whales.
626 *Marine Ecology Progress Series*, **264**, 123-135.
- 627 Bennett, A.F. & Denman, K.L. (1985) Phytoplankton patchiness: inferences from particle statistics.
628 *Journal of Marine Research*, **43**, 307-335.
- 629 Benoit-Bird, K.J., Battaile, B.C., Heppell, S.A., Hoover, B., Irons, D., Jones, N., Kuletz, K.J., Nordstrom, C.A.,
630 Paredes, R. & Suryan, R.M. (2013) Prey Patch Patterns Predict Habitat Use by Top Marine
631 Predators with Diverse Foraging Strategies. *Plos One*, **8**, e53348.
- 632 Benoit-Bird, K.J., Waluk, C.M. & Ryan, J.P. (2019) Forage Species Swarm in Response to Coastal
633 Upwelling. *Geophysical Research Letters*, **46**, 1537-1546.
- 634 Benoit-Bird, K.J., Moline, M.A. & Southall, B.L. (2017) Prey in oceanic sound scattering layers organize to
635 get a little help from their friends. *Limnology and Oceanography*, **62**, 2788-2798.
- 636 Benson, S.R., Croll, D.A., Marinovic, B.B., Chavez, F.P. & Harvey, J.T. (2002) Changes in the cetacean
637 assemblage of a coastal upwelling ecosystem during El Niño 1997–98 and La Niña 1999. *Progress
638 in Oceanography*, **54**, 279-291.
- 639 Bruce, W. (1915) Some observations on Antarctic cetacea. *Scotia Natl. Antarct. Exped. Rep*, **4**, 491-505.
- 640 Cade, D.E., Carey, N., Domenici, P., Potvin, J. & Goldbogen, J.A. (2020) Predator-informed looming
641 stimulus experiments reveal how large filter feeding whales capture highly maneuverable forage
642 fish. *Proceedings of the National Academy of Sciences*, **117**, 472-478.
- 643 Cade, D.E., Friedlaender, A.S., Calambokidis, J. & Goldbogen, J.A. (2016) Kinematic Diversity in Rorqual
644 Whale Feeding Mechanisms. *Current Biology*, **26**, 2617-2624.

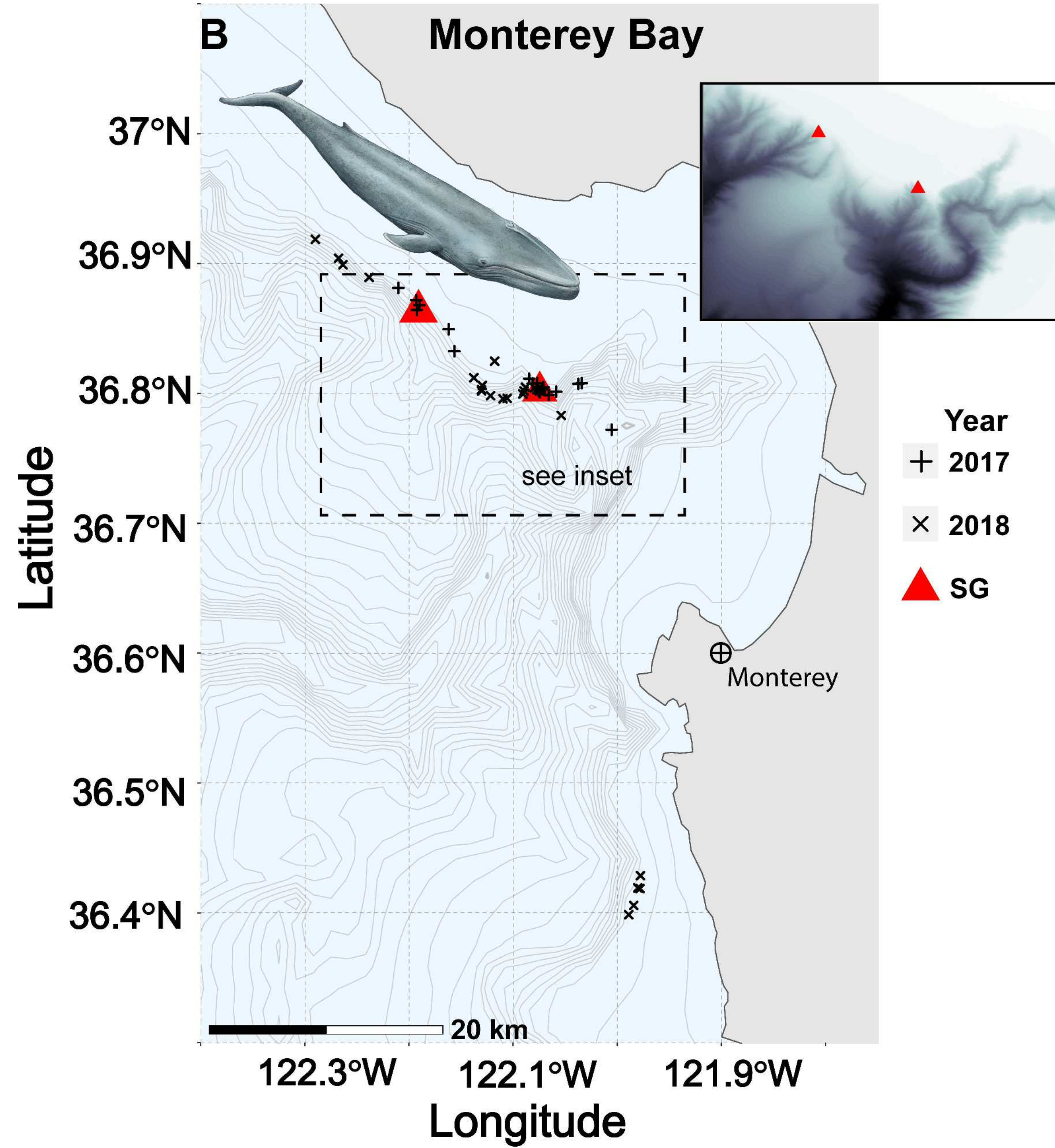
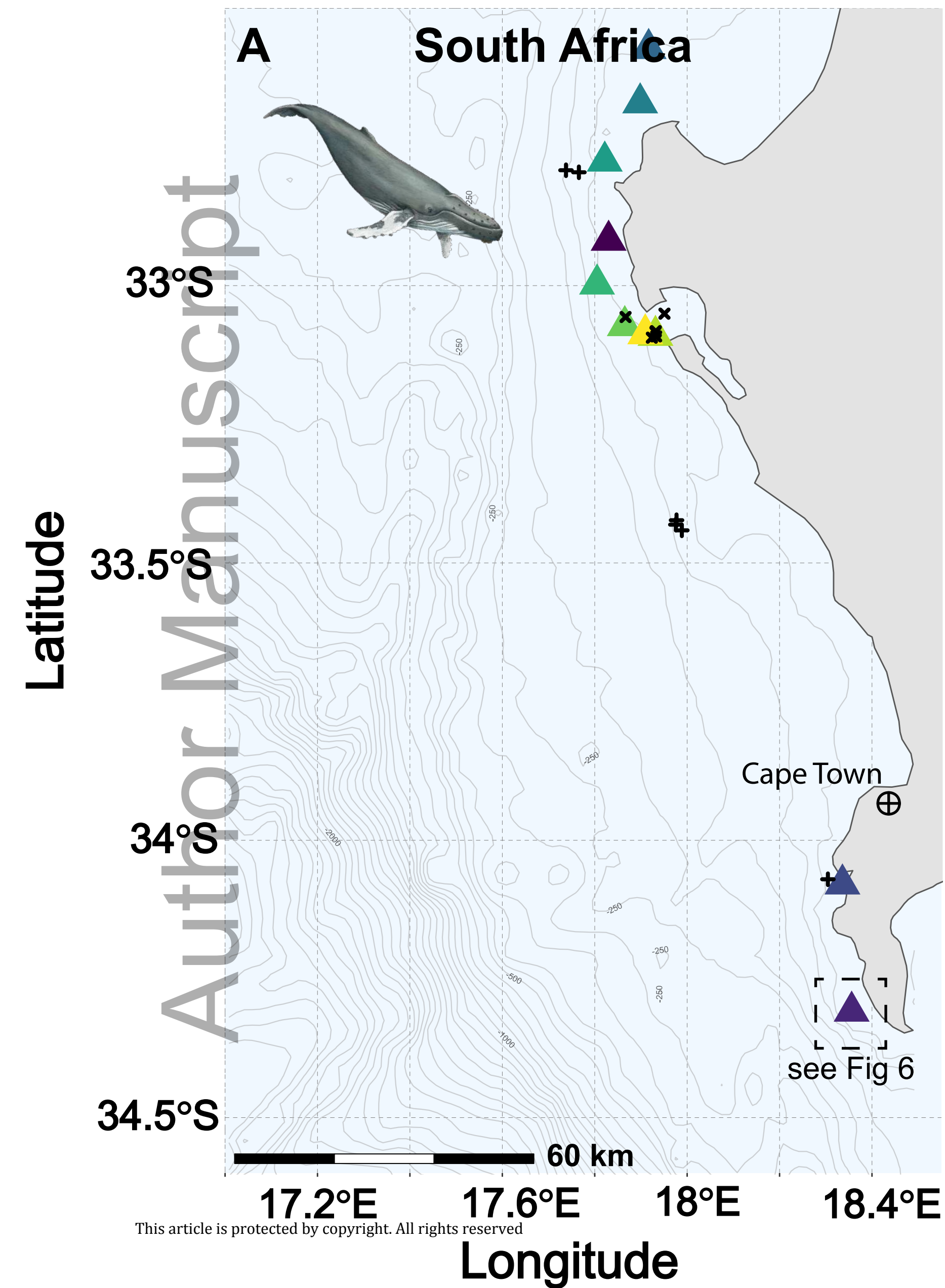
- 645 Campbell, J.W. (1995) The lognormal distribution as a model for bio-optical variability in the sea. *Journal*
646 *of Geophysical Research: Oceans*, **100**, 13237-13254.
- 647 Chave, J. (2013) The problem of pattern and scale in ecology: what have we learned in 20 years? *Ecology*
648 *Letters*, **16**, 4-16.
- 649 Coetzee, J. (2000) Use of a shoal analysis and patch estimation system (SHAPES) to characterise sardine
650 schools. *Aquatic Living Resources*, **13**, 1-10.
- 651 Cotté, C. & Simard, Y. (2005) Formation of dense krill patches under tidal forcing at whale feeding hot
652 spots in the St. Lawrence Estuary. *Marine Ecology Progress Series*, **288**, 199-210.
- 653 Cox, M.J., Demer, D.A., Warren, J.D., Cutter, G.R. & Brierley, A.S. (2009) Multibeam echosounder
654 observations reveal interactions between Antarctic krill and air-breathing predators. *Marine*
655 *Ecology Progress Series*, **378**, 199-209.
- 656 Croll, D.A., Tershy, B.R., Hewitt, R.P., Demer, D.A., Fiedler, P.C., Smith, S.E., Armstrong, W., Popp, J.M.,
657 Kiekhefer, T. & Lopez, V.R. (1998) An integrated approach to the foraging ecology of marine birds
658 and mammals. *Deep Sea Research Part II: Topical Studies in Oceanography*, **45**, 1353-1371.
- 659 Dennis, B. & Patil, G.P. (1987) Applications in Ecology. *Lognormal distributions* (eds E.L. Crow & K.
660 Shimizu), pp. 303-330. Marcel Dekker New York.
- 661 Feyrer, L.J. & Duffus, D.A. (2015) Threshold foraging by gray whales in response to fine scale variations in
662 mysid density. *Marine Mammal Science*, **31**, 560-578.
- 663 Findlay, K.P., Seakamela, S.M., Meyer, M.A., Kirkman, S.P., Barendse, J., Cade, D.E., Hurwitz, D.,
664 Kennedy, A., Kotze, P.G.H., McCue, S.A., Thornton, M., Vargas-Fonseca, O.A. & Wilke, C.G.
665 (2017) Humpback whale “super-groups” – A novel low-latitude feeding behaviour of Southern
666 Hemisphere humpback whales (*Megaptera novaeangliae*) in the Benguela Upwelling System.
667 *PLoS ONE*, **12**, e0172002.
- 668 Fossette, S., Abrahms, B., Hazen, E.L., Bograd, S.J., Zilliacus, K.M., Calambokidis, J., Burrows, J.A.,
669 Goldbogen, J.A., Harvey, J.T., Marinovic, B., Tershy, B.R. & Croll, D.A. (2017) Resource
670 partitioning facilitates coexistence in sympatric cetaceans in the California Current. *Ecology and*
671 *evolution*, **7**, 9085-9097.
- 672 Giraldeau, L.-A. & Caraco, T. (2000) Ch 8- Social Patch and Prey Models. *Social Foraging Theory*.
673 Princeton University Press, Princeton, NJ, USA.
- 674 Goldbogen, J.A., Cade, D.E., Calambokidis, J., Friedlaender, A.S., Potvin, J., Segre, P.S. & Werth, A.J.
675 (2017) How Baleen Whales Feed: The Biomechanics of Engulfment and Filtration. *Annual review*
676 *of marine science*, **9**, 1-20.

- 677 Goldbogen, J.A., Cade, D.E., Wisniewska, D.M., Potvin, J., Segre, P.S., Savoca, M.S., Hazen, E.L.,
678 Czapanskiy, M.F., Kahane-Rappoport, S.R., DeRuiter, S.L., Gero, S., Tønnesen, P., Gough, W.T.,
679 Hanson, M.B., Holt, M., Jensen, F.H., Simon, M., Stimpert, A.K., Arranz, P., Johnston, D.W.,
680 Nowacek, D.P., Parks, S.E., Visser, F., Friedlaender, A.S., Tyack, P.L., Madsen, P.T. & Pyenson,
681 N.D. (2019) Why whales are big but not bigger: Physiological drivers and ecological limits in the
682 age of ocean giants. *Science*, **366**, 1367-1372.
- 683 Goldbogen, J.A., Calambokidis, J., Croll, D.A., Harvey, J.T., Newton, K.M., Oleson, E.M., Schorr, G. &
684 Shadwick, R.E. (2008) Foraging behavior of humpback whales: kinematic and respiratory
685 patterns suggest a high cost for a lunge. *Journal of Experimental Biology*, **211**, 3712-3719.
- 686 Goldbogen, J.A., Calambokidis, J., Croll, D.A., McKenna, M.F., Oleson, E., Potvin, J., Pyenson, N.D., Schorr,
687 G., Shadwick, R.E. & Tershy, B.R. (2012) Scaling of lunge-feeding performance in rorqual whales:
688 mass-specific energy expenditure increases with body size and progressively limits diving
689 capacity. *Functional Ecology*, **26**, 216-226.
- 690 Gordon, D.M. (2014) The ecology of collective behavior. *PLoS Biology*, **12**, e1001805.
- 691 Guilpin, M., Lesage, V., McQuinn, I., Goldbogen, J.A., Potvin, J., Jeanniard-du-Dot, T., Doniol-Valcroze, T.,
692 Michaud, R., Moisan, M. & Winkler, G. (2019) Foraging energetics and prey density
693 requirements of western North Atlantic blue whales in the Estuary and Gulf of St. Lawrence,
694 Canada. *Marine Ecology Progress Series*, **625**, 205-223.
- 695 Hazen, E.L., Friedlaender, A.S. & Goldbogen, J.A. (2015) Blue whale (*Balaenoptera musculus*) optimize
696 foraging efficiency by balancing oxygen use and energy gain as a function of prey density.
697 *Science Advances*, **1**, e1500469.
- 698 Hazen, E.L., Friedlaender, A.S., Thompson, M.A., Ware, C.R., Weinrich, M.T., Halpin, P.N. & Wiley, D.N.
699 (2009) Fine-scale prey aggregations and foraging ecology of humpback whales *Megaptera*
700 *novaeangliae*. *Marine Ecology Progress Series*, **395**, 75-89.
- 701 Hein, A.M., Altshuler, D.L., Cade, D.E., Liao, J.C., Martin, B.T. & Taylor, G.K. (2020) An Algorithmic
702 Approach to Natural Behavior. *Current Biology*, **30**, R663–R667.
- 703 Hein, A.M. & Martin, B.T. (2020) Information limitation and the dynamics of coupled ecological systems.
704 *Nature Ecology & Evolution*, **4**, 82-90.
- 705 Jaquet, N. (1996) Distribution and spatial organization of groups of sperm whales in relation to biological
706 and environmental factors in the South Pacific.
- 707 Jarvis, T., Kelly, N., Kawaguchi, S., van Wijk, E. & Nicol, S. (2010) Acoustic characterisation of the broad-
708 scale distribution and abundance of Antarctic krill (*Euphausia superba*) off East Antarctica (30-80

- 709 E) in January-March 2006. *Deep Sea Research Part II: Topical Studies in Oceanography*, **57**, 916-
710 933.
- 711 Jurasz, C.M. & Jurasz, V.P. (1979) Feeding modes of the humpback whale (*Megaptera Novaeangliae*) in
712 southeast Alaska. *Scientific Reporting of Whales Research Institute*, **31**, 69-83.
- 713 Kaartvedt, S., Røstad, A., Fiksen, Ø., Melle, W., Torgersen, T., Breien, M.T. & Klevjer, T.A. (2005)
714 Piscivorous fish patrol krill swarms. *Marine Ecology Progress Series*, **299**, 1-5.
- 715 Kahane-Rapport, S.R. & Goldbogen, J.A. (2018) Allometric scaling of morphology and engulfment
716 capacity in rorqual whales. *Journal of Morphology*, 1-13.
- 717 Kirchner, T., Wiley, D.N., Hazen, E.L., Parks, S.E., Torres, L.G. & Friedlaender, A.S. (2018) Hierarchical
718 foraging movement of humpback whales relative to the structure of their prey. *Marine Ecology
719 Progress Series*, **607**, 237-250.
- 720 LaScala-Gruenewald, D.E., Mehta, R.S., Liu, Y. & Denny, M.W. (2019) Sensory perception plays a larger
721 role in foraging efficiency than heavy-tailed movement strategies. *Ecological Modelling*, **404**, 69-
722 82.
- 723 Leibniz, G. (1684) A new method for maxima and minima as well as tangents, which is neither impeded
724 by fractional nor irrational quantities, and a remarkable type of calculus for them (*translation*).
725 *A Source Book in Mathematics, 1200–1800 (Struik, D. J.)*. pp. 271-281. Harvard University Press.
- 726 Levin, S.A. (1992) The problem of pattern and scale in ecology: the Robert H. MacArthur award lecture.
727 *Ecology*, **73**, 1943-1967.
- 728 MacLennan, D.N., Fernandes, P.G. & Dalen, J. (2002) A consistent approach to definitions and symbols in
729 fisheries acoustics. *ICES Journal of Marine Science*, **59**, 365-369.
- 730 Magurran, A.E. & Henderson, P.A. (2003) Explaining the excess of rare species in natural species
731 abundance distributions. *Nature*, **422**, 714-716.
- 732 Mann, J. (2000) Unraveling the dynamics of social life. *Cetacean societies: field studies of dolphins and
733 whales*. (eds J. Mann, R.C. Connor, P. Tyack & H. Whitehead), pp. 45-64. University of Chicago
734 Press, , Chicago, Illinois, USA.
- 735 Mastick, N. (2016) The Effect of Group Size on Individual Roles and the Potential for Cooperation in
736 Group Bubble-net Feeding Humpback Whales (*Megaptera novaeangliae*). M.S., Oregon State
737 University.
- 738 Mayo, C.A. & Marx, M.K. (1990) Surface foraging behaviour of the North Atlantic right whale, *Eubalaena
739 glacialis*, and associated zooplankton characteristics. *Canadian Journal of Zoology*, **68**, 2214-
740 2220.

- 741 Nickels, C.F., Sala, L.M. & Ohman, M.D. (2019) The euphausiid prey field for blue whales around a steep
742 bathymetric feature in the southern California current system. *Limnology and Oceanography*,
743 **64**, 390-405.
- 744 Nicol, S., James, A. & Pitcher, G. (1987) A first record of daytime surface swarming by *Euphausia lucens*
745 in the Southern Benguela region. *Marine Biology*, **94**, 7-10.
- 746 Nowacek, D.P., Friedlaender, A.S., Halpin, P.N., Hazen, E.L., Johnston, D.W., Read, A.J., Espinasse, B.,
747 Zhou, M. & Zhu, Y. (2011) Super-aggregations of krill and humpback whales in Wilhelmina Bay,
748 Antarctic Peninsula. *PLoS One*, **6**, e19173.
- 749 Owen, K., Kavanagh, A.S., Warren, J.D., Noad, M.J., Donnelly, D., Goldizen, A.W. & Dunlop, R.A. (2017)
750 Potential energy gain by whales outside of the Antarctic: prey preferences and consumption
751 rates of migrating humpback whales (*Megaptera novaeangliae*). *Polar Biology*, **40**, 277-289.
- 752 Pagel, M.D., Harvey, P.H. & Godfray, H. (1991) Species-abundance, biomass, and resource-use
753 distributions. *The American Naturalist*, **138**, 836-850.
- 754 Piatt, J.F. & Methven, D.A. (1992) Threshold foraging behavior of baleen whales. *Marine Ecology*
755 *Progress Series*, **84**, 205-210.
- 756 Pivorunas, A. (1979) The Feeding Mechanisms of Baleen Whales. *American Scientist*, **67**, 432-440.
- 757 Preston, F.W. (1948) The commonness, and rarity, of species. *Ecology*, **29**, 254-283.
- 758 Preston, F.W. (1962) The canonical distribution of commonness and rarity: Part I. *Ecology*, **43**, 185-215.
- 759 Przybylski, A.K., Murayama, K., DeHaan, C.R. & Gladwell, V. (2013) Motivational, emotional, and
760 behavioral correlates of fear of missing out. *Computers in Human Behavior*, **29**, 1841-1848.
- 761 Rocha, R.C., Clapham, P.J. & Ivashchenko, Y.V. (2014) Emptying the oceans: a summary of industrial
762 whaling catches in the 20th century. *Marine Fisheries Review*, **76**, 37-48.
- 763 Santora, J.A., Zeno, R., Dorman, J.G. & Sydeman, W.J. (2018) Submarine canyons represent an essential
764 habitat network for krill hotspots in a large marine ecosystem. *Scientific reports*, **8**, 7579.
- 765 Slater, G.J., Goldbogen, J.A. & Pyenson, N.D. (2017) Independent evolution of baleen whale gigantism
766 linked to Plio-Pleistocene ocean dynamics. *Proc. R. Soc. B*, **284**, 20170546.
- 767 Southall, B.L., DeRuiter, S.L., Friedlaender, A., Stimpert, A.K., Goldbogen, J.A., Hazen, E., Casey, C.,
768 Fregosi, S., Cade, D.E. & Allen, A.N. (2019) Behavioral responses of individual blue whales
769 (*Balaenoptera musculus*) to mid-frequency military sonar. *Journal of Experimental Biology*, **222**,
770 jeb190637.
- 771 Stephens, D.W. & Krebs, J.R. (1986) *Foraging theory*. Princeton University Press.

- 772 van der Hoop, J., Nousek-McGregor, A., Nowacek, D., Parks, S., Tyack, P. & Madsen, P. (2019) Foraging
773 rates of ram-filtering North Atlantic right whales. *Functional Ecology*, **33**, 1290-1306.
- 774 Watkins, J.L. & Murray, A.W.A. (1998) Layers of Antarctic krill, *Euphausia superba*: are they just long krill
775 swarms? *Marine Biology*, **131**, 237-247.
- 776 White, G.C. (1978) Estimation of plant biomass from quadrat data using the lognormal distribution.
777 *Journal of Range Management*, 118-120.
- 778 Whitehead, H. (1983) Structure and stability of humpback whale groups off Newfoundland. *Canadian*
779 *Journal of Zoology*, **61**, 1391-1397.
- 780 Wiley, D.N., Ware, C., Bocconcelli, A., Cholewiak, D., Friedlaender, A., Thompson, M. & Weinrich, M.
781 (2011) Underwater components of humpback whale bubble-net feeding behavior. *Behaviour*,
782 **148**, 575-602.
- 783 Wilson, R.P., Neate, A., Holton, M.D., Shepard, E.L., Scantlebury, D.M., Lambertucci, S.A., di Virgilio, A.,
784 Crooks, E., Mulvenna, C. & Marks, N. (2018) Luck in food finding affects individual performance
785 and population trajectories. *Current Biology*, **28**, 3871-3877. e3875.
- 786

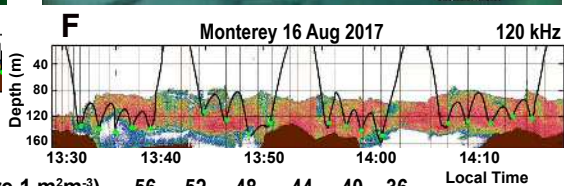




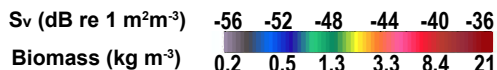
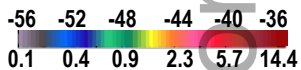
Surface observations



Whale-borne video & 3d accelerometry

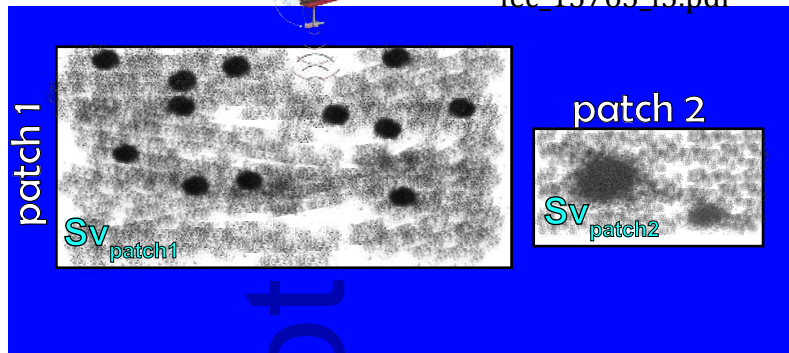


Acoustic prey mapping



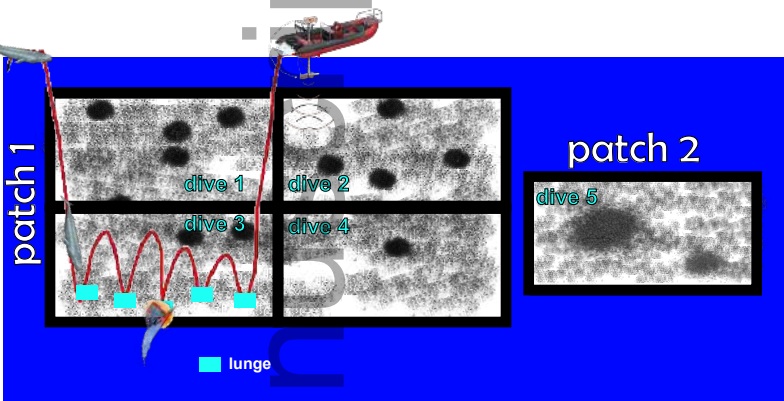
A

Patch identification

Patch 1
acoustic
energy : Sv_{patch1} ↓
*Biomass
Conversion* B_{patch1}
($kg\ m^{-3}$)Patch 2
acoustic
energy : Sv_{patch2} ↓
*Biomass
Conversion* B_{patch2}
($kg\ m^{-3}$)

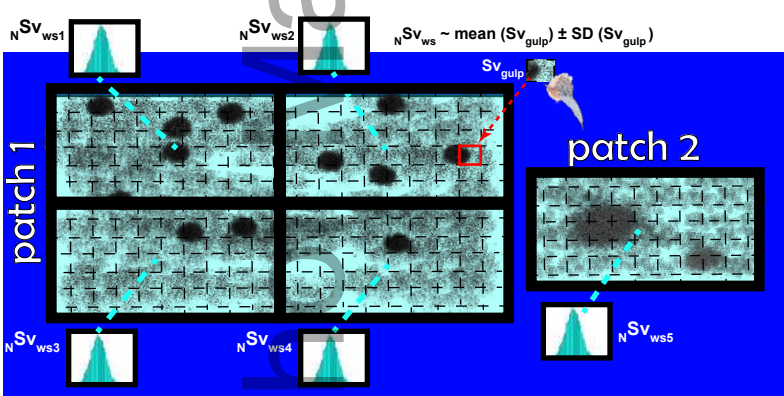
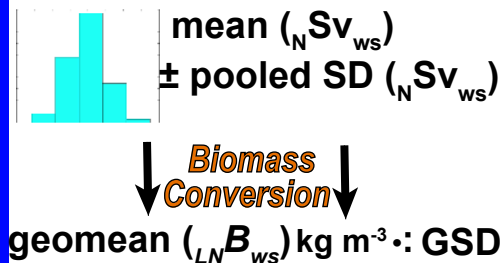
B

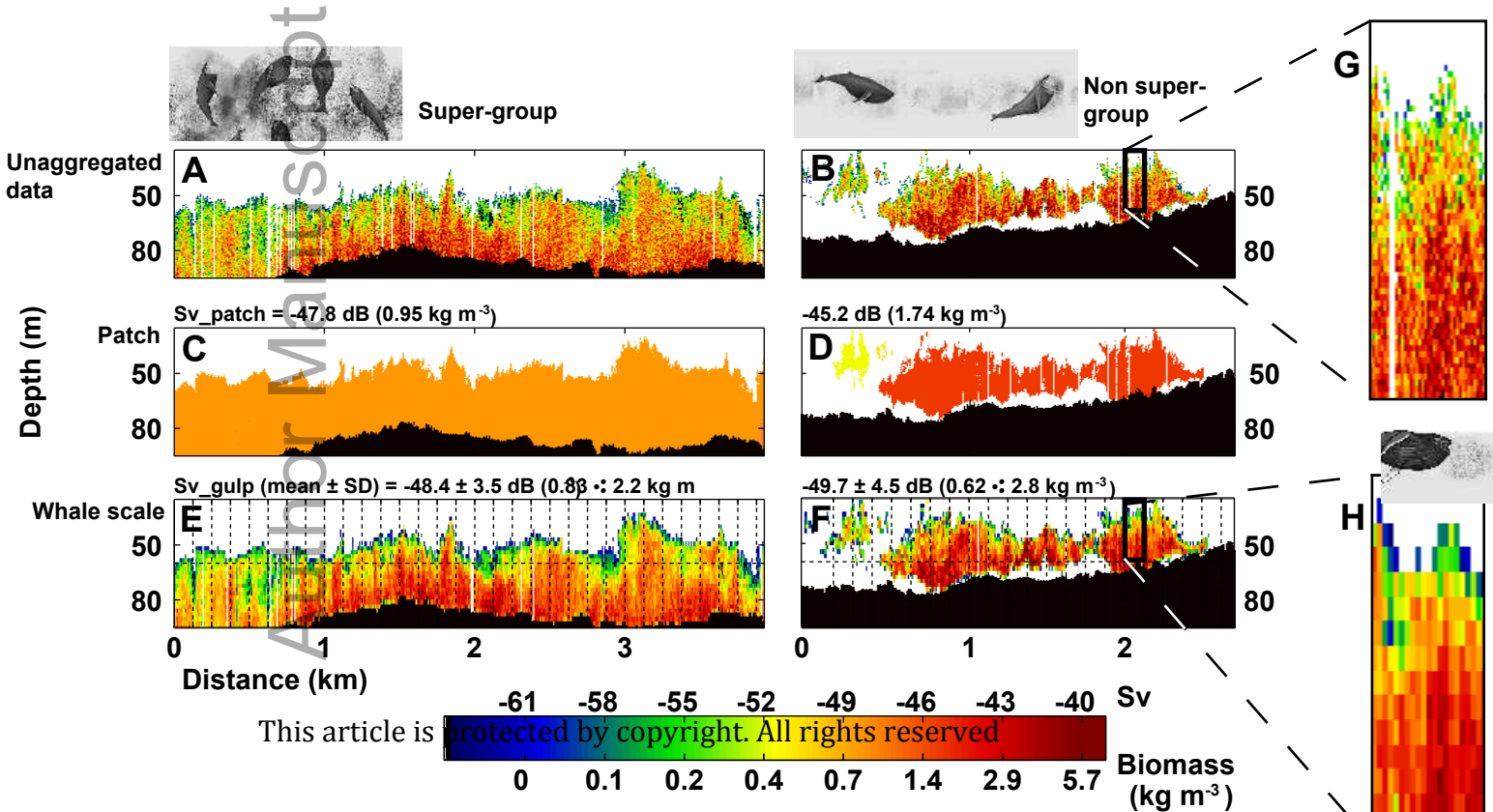
Dive-sized cells



C

Whale scale

Mean biomass
availability at the
whale scale



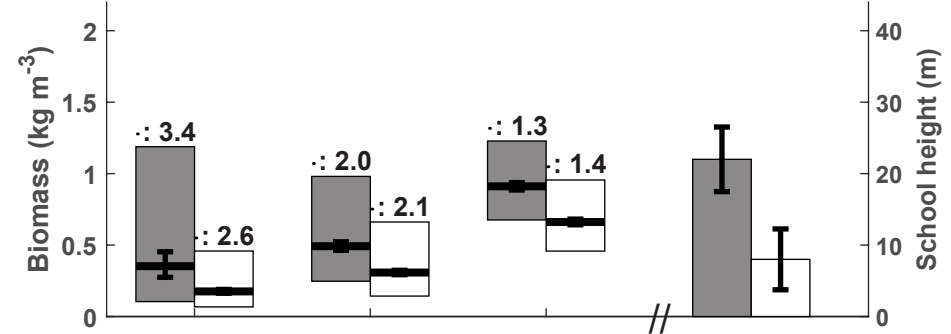
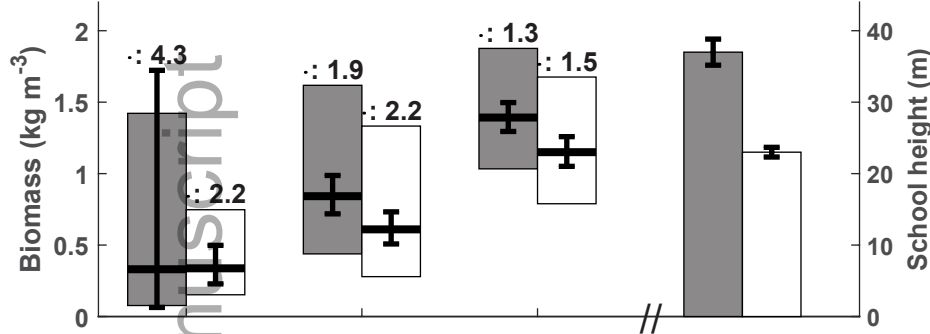
Example Day

fec_13763_f5.pdf
 SG
 NSG

Summary (all days combined)

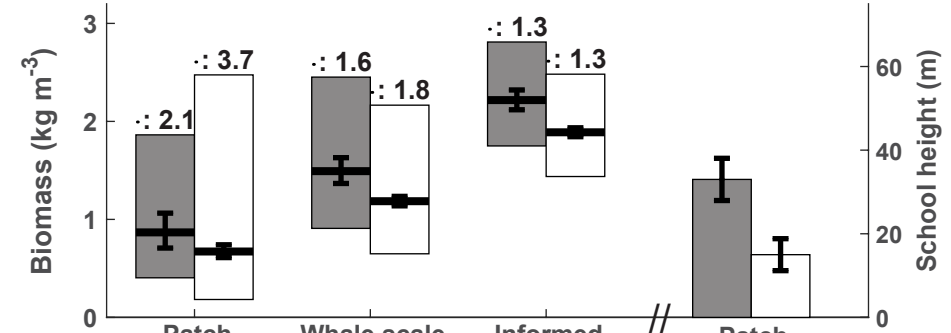
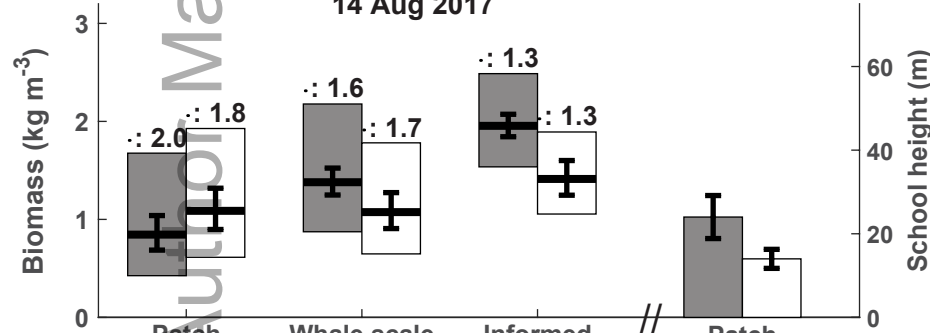
South Africa

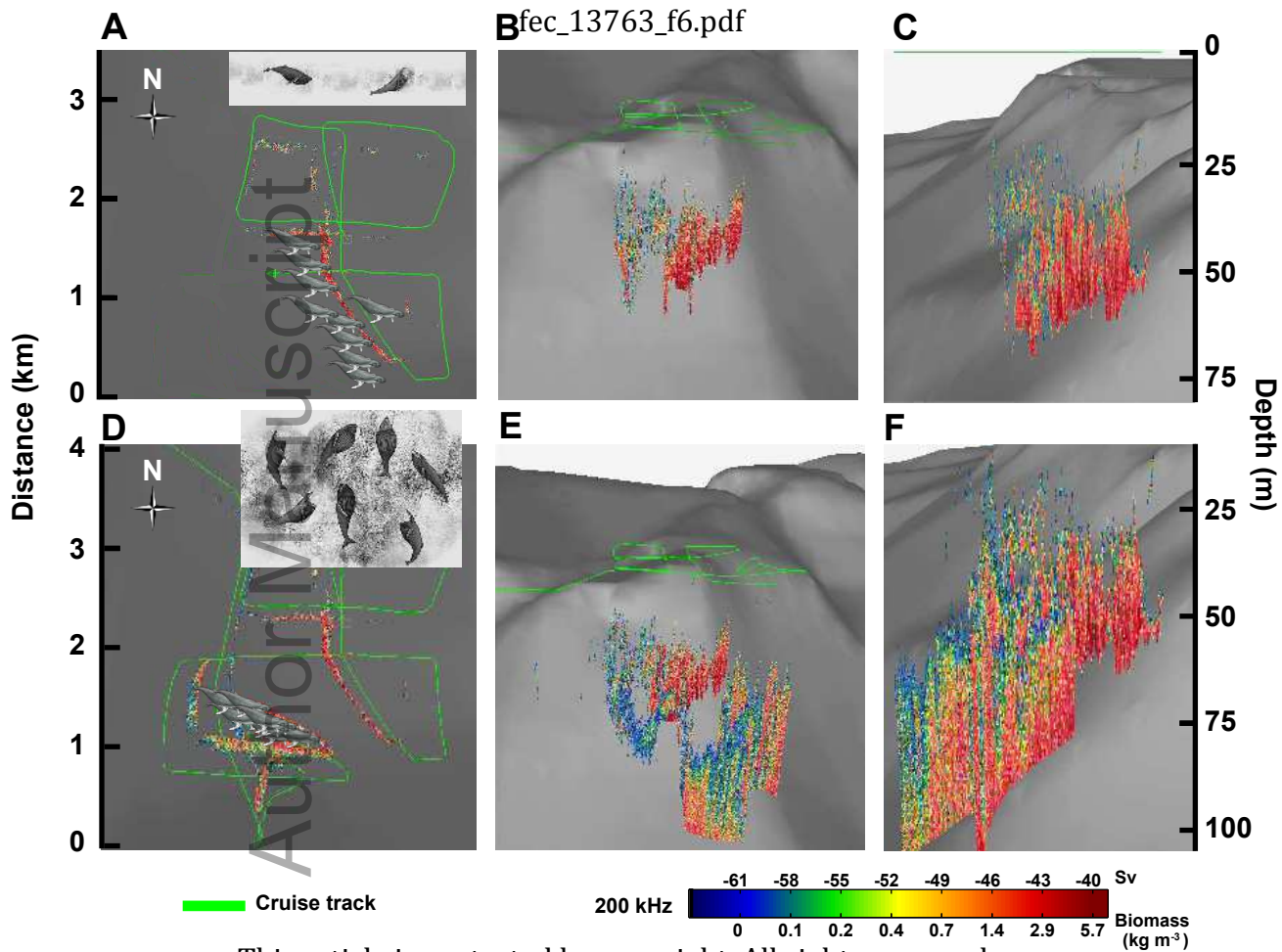
05 Nov 2015



Monterey

14 Aug 2017

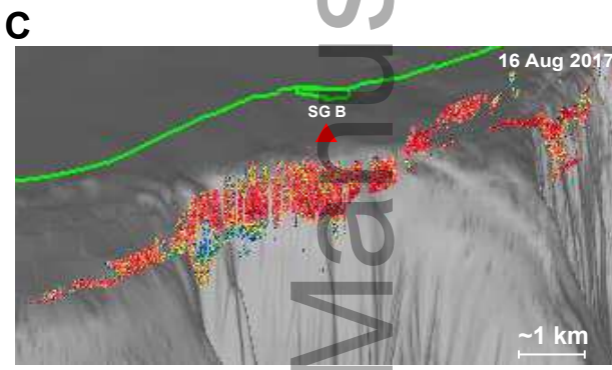
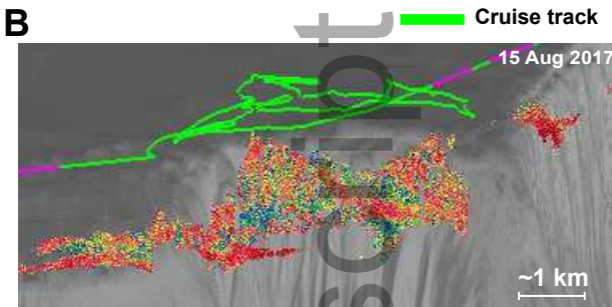
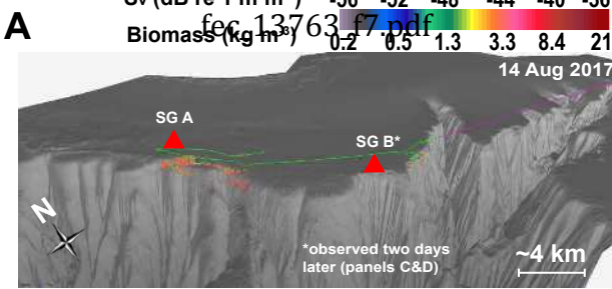




This article is protected by copyright. All rights reserved

Sv (dB re 1 m²m⁻³) -56 -52 -48 -44 -40 -36

Biomass (kg m⁻³) 0.2 0.5 1.3 3.3 8.4 21



- D**
- bw170816-42
 - bw170816-44
 - bw170816-51
 - bw170816-23
 - Lunge feeding event
-

